MODELING THE PECAN NUT GROWTH AND CARBOHYDRATE REQUIREMENT AND APPLICATION OF MODELS

By

SRIJANA PANTA

Bachelor of Science in Agriculture

Tribhuvan University

Kathmandu, Nepal

2018

Submitted to the Faculty of the
Graduate College of the
Oklahoma State University
in partial fulfillment of
the requirements for
the Degree of
MASTER OF SCIENCE
December, 2021

MODELING THE PECAN NUT GROWTH AND

CARBOHYDRATE REQUIREMENT AND

APPLICATION OF MODELS

Thesis Approved:

Dr. Lu Zhang

Thesis Adviser

Dr. Charles Fontanier

Dr. Saleh Taghvaeian

ACKNOWLEDGEMENTS

First and foremost, I would like to express my utmost gratitude to my advisor Dr. Lu Zhang who gave me the opportunity to conduct this wonderful project and provided invaluable guidance throughout this research. Her dynamism, benevolence, patience, intelligence, and sincerity have deeply inspired me. Being an international student, I couldn't have imagined having a better advisor and mentor like you. Besides, I would like to offer my special thanks to my committee members Dr. Charles Fontanier and Dr. Saleh Taghvaeian for their valuable suggestions and contributions during my research. My special thanks go to Dr. Lan Zhu and Biting Zhou for helping me with statistical analysis. I am thankful to Dr. Phil Mulder, Kelly Seuhs, Dr. Charles Rohla, Lucas Fideles Costa and Dr Yiannis Ampatzidis for their immense support in my research project.

Furthermore, I would also like express gratitude toward senior agriculturist Becky Cherry, Amandeep Kaur and Yanwei Sun for their immense help throughout my entire data collection and sample processing. Also, I appreciate the help and assistance I received from other graduate students and from entire Horticulture and Landscape Architecture Department.

To all my friends, Nikee, Kumar, Pratistha, Sanju and specially my boyfriend Abishkar Regmi for their love and support throughout out my graduate life. Last, but definitely not the least, I am greatly indebted to my family for their unconditional love and support in the these very intense academic years. My heartfelt thanks.

Name: SRIJANA PANTA

Date of Degree: DECEMBER, 2021

Title of Study: MODELING THE PECAN NUT GROWTH AND CARBOHYDRATE REQUIREMENT AND APPLICATION OF MODELS

Major Field: HORTICULTURE

Abstract: The pecan nut is an important nut fruit in the USA economy, contributing more than $3.5 billion to the country's economy. The optimal time of different orchard activities like irrigation management, pesticide spray, and harvest time is difficult to identify. The growth and development of nuts as a function of heat units can be modeled to optimally time orchard activities according to a biological calendar. Our objective was to compare various nonlinear growth models and determine which best fit pecan nut development (i.e., embryo, shell, and shuck). Gompertz and Logistic functions were fitted to the pecan data. The models were fitted separately for each environment (year × location) using data collected at 4 locations in 2019 and 1 in 2020. For 2019, each location resulted in shuck and embryo development having the best fit using the Gompertz model, while the shell development was best using a logistic model. In contrast, in 2019 and 2020 with one location, Gompertz best fits embryo and logistic for shell and shuck development. This information will aid in the development of online producer tools. Pecans are reported to have alternate or masting phenomena because of irregular nut production, which is believed to be caused by carbohydrate depletion. The nonstructural carbohydrate concentration of wood and bark was determined throughout the growing season in 2019 and 2020. We found the current season shoot supports growth of the nut, while the one- year old shoot stores reserves each following year. Our result showed that there is difference in carbohydrate concentration between two years. Low starch concentration throughout the thousands of samples tested implies there could be more than two years of low production and indicate that pecan might have a masting phenomenon. Additional research was carried out to assess pecan response to varying irrigation levels. Nut size was influenced by water stress, but this response varied with cultivar. For shell hardening, the research objective was to determine how shell hardening restricts the weevil infection. The result showed that the weevil oviposits mainly in the suture where the hardness is less. Furthermore, there was a difference in the hardness of the shell among the variety. This information will be helpful in or breeder to increase tolerance or avoidance of the pest.
Keywords: Nonlinear, Gompertz, carbohydrate, irrigation, pecan

TABLE OF CONTENTS

Chapter Page

I. SELECTING NON-LINEAR MIXED EFFECT MODEL FOR GROWTH AND DEVELOPMENT OF PECAN NUT FITTED SEPARATELY FOR TWO DIFFERENT YEAR……………………………………………………………………………………...1

Abstract………………………………………………………………………………..1
Introduction……………………………………………………………………………1
Materials and method
Location and cultivar…………………………………………………………...5
Nut measurement……………………………………………………………….6
Thermal unit…………………………………………………………………….7
Model…………………………………………………………………………...7
Growth function………………………………………………………….8
Multilevel nonlinear mixed effect model…………………………………...9

Result
Development of embryo, shell and shuck………………………………………..10
Model comparison and selection for year 2019 with different location…………11
Testing the assumption of selected nonlinear mixed model fitted to pecan nut growth data collected in 2019 with different location……………………….12
Predict growth curves with data collected in 2019 with different locations ……………………………………………………………………………………….12
Model comparison and selection for year 2019 and 2020 with one location……12
Testing the assumption of selected nonlinear mixed model fitted to pecan nut growth data collected in 2019 and 2020 with one location………………….13
Predicted growth curves for year 2019 and 2020 with one location………13
Discussion……………………………………………………………………………14
Conclusion…………………………………………………………………………...14

Chapter Page

II. SEASONAL CARBOHYDRATE BUDGET OF PECAN DURING THE FRUITING SEASON……………………………………………………………………………40

Abstract……………………………………………………………………………40
Introduction…………………………………………………………………………..41
Material and method
Sample collection……………………………………………………………...45
Sugar and starch quantification………………………………………………..45
Data analysis…………………………………………………………………..46

Result
ANOVA result…………………………………………………………………...47
Soluble sugar concentration in year 2019 and 2020……………………………..47
Soluble sugar concentration in year 2019 and 2020……………………………..48

Discussion……………………………………………………………………………48
Conclusion…………………………………………………………………………...51

Chapter Page

III. IRRIGATION AND WEEVIL MANAGEMENT: DEVELOPING PRACTICAL APPLICATIONS BASED ON THE PECAN NUT GROWTH MODEL…………........61

Abstract…………………………………………………………………………………61
Introduction……………………………………………………………………………..62
Method
Water potential test……………………………………………………………………..65
Shell firmness test………………………………………………………………..65
Data analysis……………………………………………………………………..66
Result and Discussion
Irrigation
Water potential…………………………………………………………..66
Nut growth……………………………………………………………...67
Shell firmness…………………………………………………………...67
Shell firmness of nut affected by weevil…………………………………………69
Conclusion……………………………………………………………………………...70

REFERENCES……………………………………………………………………………..82

LIST OF TABLES

Table Page

1.1. Summary of fitted models and goodness-of-fit statistics for year 2019 based on data collected multiple sites in Oklahoma. 24

1.2. Coefficient of determination (R-square) and Akaike's Information Criterion (AIC) for Logistic and Gompertz models to predict shuck, shell and embryo area; based on data collected in 2019 at multiple sites in Oklahoma. 25

1.3. Summary of fitted models and goodness-of-fit statistics for the data collected in Perkins location during 2019 and 2020 32

1.4. Coefficient of determination (R-square) and Akaike's Information Criterion (AIC) for Logistic and Gompertz models to predict shuck, shell and embryo area; based on data collected in 2019 and 2020 at Perkins location in Oklahoma. 33

2.1. ANOVA for sugar concentration for year 2019 and 2020 for variety Pawnee and Kanza in bark and wood tissue for three different seasons (Cs, 1-Yr, and 2-Yr)………..55

2.2. ANOVA for starch concentration for year 2019 and 2020 for variety Pawnee and Kanza in bark and wood tissue for three different seasons (Cs, 1-Yr, and 2-Yr) 56

Table Page

3.1. Analysis of variance for the area of the Pawnee and Kanza nut tested for different kind of irrigation treatment……….…………………………………………………...75

3.2. LSD test for the Kanza area for different kind of irrigation treatment 76

3.3. ANOVA for the firmness of the Pawnee and Kanza nut tested for full, half and no irrigation.. 77

LIST OF FIGURES

Figure Page

1.1. Images collected for the neural network training and evaluation. ‘Pawnee’ cultivar from Perkins location: (a) small (before beginning of water stage) and (b) big stages (beginning of water stage) (Costa et al., 2021). 21

1.2. Growth curve of (a)shuck, (b) shell and (c) embryo development of Pawnee and Kanza cultivar of year 2019 and 2020. Red curve is for development of Kanza whereas blue is for Pawnee cultivar. The x-axis is the thermal unit (tu) calculated from bloom until harvest. The y-axis is the area of nut component (shuck, shell and embryo) in mm^2. Each dot in the graph represent the average area of the respective component of three replications for a single cultivar collected in each sampling date... 23

1.3. Residuals (observed - predicted) for fitted Gompertz [embryo (a) and shuck (c)], and Logistic [shell (b)] model fitted to pecan nut growth data collected in 2019 along with different location. 27

1.4. QQ plots for Gompertz (embryo (a) and shuck (c)) and Logistic (shell (b)) model fitted to pecan nut growth data collected in 2019 along with different location. 29

Figure Page

1.5. Non-linear mixed model for (a) embryo, (b) shell and (c) shuck with different location in year 2019. The solid line in the graph is for the beginning of water stage of nut, dot dash line is for beginning of gel stage and dashed line is for beginning of dough. The red line curve represents the population average which is fitted by the model by considering location as a random effect whereas the blue dotted line curve is the subject specific which consider cultivar as a fixed effect.. 31

1.6. Residuals (observed - predicted) for Gompertz (embryo (a)) and Logistic (shell (b) and shuck (c)) model fitted to pecan nut growth data collected in 2019 and 2020 for one location 35

1.7. QQ plots for Logistic (shell (a)) model, and Gompertz (shuck (b) and embryo (c)) model fitted to pecan nut growth data collected in 2019 and 2020 for one location 37

1.8. Non-linear mixed model for a) shuck, b) shell and c) embryo with of Perkins in year 2019 and 2020. The solid line in the graph is for the beginning of water stage of nut, dot dash line is for beginning of gel stage and dashed line is for beginning of dough. The red curve represents the population average growth curve for each cultivar whereas the blue dotted curve is the subject specific growth curve for the cultivar at different year. The two type of lines are all estimated by the same non-linear mixed effect model.. 39

2.1. Brach showing each section; Current season (Cs), one-year old (1-Yr) and two year old (2-Yr) 54

Figure Page

2.2. Average sugar content (±Standard error) in Pawnee and Kanza bark during 2019 and 2020 a) Pawnee bark 2019, b) Pawnee wood 2019, c) Pawnee bark 2020, d) Pawnee wood 2020, e) Kanza bark 2019, f) Kanza wood 2019, g) Kanza bark 2020, and h) Kanza wood 2020. Different line in the graph is for the different season shoot i.e., blue is for Cs (Current season), red is for 1-Yr (one-year-old) and green is for 2-Yr (two-year-old) shoot. 58

2.3. Average starch content (±Standard error) in Pawnee and Kanza bark during 2019 and 2020 a) Pawnee bark 2019, b) Pawnee wood 2019, c) Pawnee bark 2020, d) Pawnee wood 2020, e) Kanza bark 2019, f) Kanza wood 2019, g) Kanza bark 2020, and h) Kanza wood 2020. Different line in the graph is for the different season shoot i.e., blue is for Cs (current season), red is for 1-Yr (one-year-old) and green is for 2-Yr (two-year-old) shoot. 60

3.1. Kanza pecan at water stage. 71

3.2. Soil moisture tension at 6'' and 30'' depths tested by WATERMARK soil moisture sensors installed at the distance to half canopy. 72

3.3. Measuring pecan shell firmness using force gauge with a 2mm probe needle. 73

3.4. Average leaf water potential (±Standard error) of Pawnee and Kanza trees tested once a week in August. Two tests in the first week. The red dots represent the full irrigation, green dots the half irrigation, and the blue is the non-irrigation. Note: water potential is a negative value; lower the negative value, higer demand for water. 74

Figure Page

3.5. Correlation between shell area and shell hardness during the Pecan nut growth for Pawnee (A to C) and Kanza (D to F) variety with different irrigation treatment; A and D (Full irrigation), B and E (Half irrigation), and C and F (No irrigation). Shaded area is the of 95% confidence interval. 78

3.6. Kanza nuts with and without shucks (a) non-sutured side on shell, the middle of the shuck has faint discolored lines; (b) sutured side on the shell, the middle of shuck has clear discolored lines; (c) from base to distal ends divided into 1, 2, 3 sections on the shuck surface without discolored line; (d) from base to distal ends divided into 4, 5, 6 sections on the surface adjacent to (Figure 3.6c) in clockwise direction; (e) from base to distal ends divided into 7, 8, 9 sections on the surface adjacent to (Figure 3.6d) in clockwise direction; from base to distal ends divided into 10,11,12 sections on the surface adjacent to (Figure 3.6e) in clockwise direction. 79

3.7. Growth curve for shell firmness with confidence interval (sections 2 or 8) of Pawnee (a) and Kanza (b) nuts collected from early fruit set July through October in 2020. 80

3.8. The mean nut firmness (±SE) (lb/2mm2) of the 12 sections of the six nuts on which the asterisk (*) indicates sections with weevil damage. Different letters indicate significant statistical differences........ 81

CHAPTER I

SELECTING NON-LINEAR MIXED EFFECT MODEL FOR GROWTH AND DEVELOPMENT OF PECAN NUT

Abstract

Pecan nut is an important fruit in the USA, contributing more than $3.5 billion to the country's economy. The optimal time of different orchard activities like irrigation management, pesticide spray, and optimal harvest time is difficult to identify. Growth and development of the nut as a function of heat unit can be used as a valuable tool to predict different growth stages of the nut. Growth models are useful tools that provide growers with useful information regarding different management activities. The objectives of this research were to compare different non-linear growth models and determine which fits the best to the growth or development of pecan nut components i.e., embryo, shell, and shuck. The sampled nuts were collected in two different years (2019 and 2020). In 2019, three varieties of nuts were sampled from five different locations. In 2020, samples of two varieties were collected from one location. Separate models were fitted for (1) the 2019 data to capture the variation among different locations and varieties and (2) the 2019 and 2020 data within one location but considering the random effect between years across two cultivars. By comparing the coefficient of determination (R^2) and Akaike information criteria (AIC) among fitted models, the Gompertz model best fits the embryo development for both datasets. It also describes the best for the growth of shuck from the 2019 data. The Logistic model performs slightly better than Gompertz for modeling shell growth for both datasets and shuck for the two-year data. A finding from our research will guide in building an integrated growth model with three phenotypic traits (shuck, shell, and embryo). Models will be made publicly available through a web tool that can predict different nut development stages of nut development for multiple orchard management practices like irrigation, thinning, and pest management.

Keywords: Nonlinear, pecan, Gompertz, Logistic

1. Introduction

Pecan [*Carya illinoiensis* (Wangenh.) K. Koch] is a deciduous nut tree native to northeastern North America (Sparks, 2005). The United States is one of the largest producers of pecan. The utilized pecan production in 2020 was 305 million pounds, and the value of utilized production was 435 million dollars (USDA-NASS, 2021). The production of pecan is erratic due to alternate bearing (Conner & Worley,2000; Sparks, 2005). Alternate bearing in pecan is enhanced by biotic (insects) and abiotic (drought or nutrient) stresses (Rohla, 2014).

The nuts are produced through the onset of flowering. Pollen is shed from catkins, which are usually high in number (up to 15 million pollen grains) whereas there are only three to six female flowers in the terminal of fruiting shoots. Each female flower of pecan has three major components i.e., stigma, style, and ovary. Exocarp, mesocarp, and endocarp are the major components of the ovary wall. Shuck (outer layer of nut) is developed from exocarp and mesocarp, while the shell is developed from endocarp. Double fertilization occurs within the ovule in which one sperm cell unites with the ovule to form a zygote while another one will unite with a special cell to form the endosperm nucleus. Later, the endosperm nucleus forms the liquid endosperm, which will provide nutrients for kernel development. Pecan nut development can be divided into two phases: Endosperm development phase (phase I) and embryo growth (phase II) (Byford, 2005; Herrera, 1990). Water stage (the time when the shell and the embryo of nut become fully sized and the embryo is filled with liquid endosperm) and gel stage (the time when the liquid endosperm solidifies and form a thick layer of gel around the embryo) occur at phase I followed by shell hardening, dough stage (filling of embryo with packing tissue), and shuck split in phase II. Mature pecan fruit is divided into three main parts: shuck (involucre), shell, and the kernel or embryo (Thompson, 1998).

Nut thinning of pecan is a commonly practiced management tool to reduce alternate bearing. Thinning is performed when the ovule at the water stage is at 50 to 100% expansion (Smith & Gallott, 1990). However, it can be difficult to predict the expansion rate. While they are too small, thinning nuts can damage the tree due to the large force of equipment, while thinning too late, (dough stage) can reduce benefits on kernel quality, return bloom, and cold hardiness (Carroll et al., 2015). Pecan nut has a unique stage called the water stage, which starts from July to August depending upon location and cultivar. This is the period where an increase in nut size takes place. Adequate rainfall during this period helps in the maximum nut elongation and expansion, whereas deficit irrigation during this stage causes minimum nut elongation and expansion (Sparks, 1995). Lack of irrigation during the nut sizing period results in fruit abortion (Sparks, 1989). A dynamic crop model which combines physiological processes and their dependencies on the environment may provide practical aid in management decision making (Dayan et al., 1993).

Similarly, another important factor affecting nut production is pest infestation. The pecan weevil is one of the critical pests of pecan, and it requires multiple insecticide applications each year to prevent economic damage (Harris, 1983). Weevils damage the nuts before and after kernel initiation by feeding or by oviposition. The weevil deposits the egg on the distal end of the developing nut, which later hatches and consumes the kernel. The weevil penetrates the nut right after the water stage, and the shell has lignified (Mulder et al., 2012). The above information reveals that it is important to study the growth rate of pecan nuts to improve orchard management practices for optimizing maximum fruit size and quality (Herrera, 1990). Predict each stage of nut growth will aid in orchard operation scheduling and efficiency and hence increase net return. Crop models provide information to farmers about crop growth and developmental stages and can be valuable tools for improving the efficiency and timing of pesticide applications, irrigation, fertilization, and scheduling harvest operations (Chmielewski, 2003; Zavalloni et al., 2006).

Temperature controls the development rate of the plant. The amount of heat or thermal time required for a plant to achieve a specific phenological stage can be expressed in terms of growing degree hour (GDH) or growing degree day (GDD) (Zavalloni et al., 2006). Growing degree hour is a valuable tool to estimate temperature accumulation which considers both time and temperature (Azarenko et al., 2008) and is calculated by the sum of temperature readings divided by number of reading used minus base temperature (Costa et al., 2021). Mimoun & DeJong (1998) described GDD as a valuable tool to predict harvest date in peach. Growing degree day is calculated based on the average of daily maximum temperature and minimum temperature minus a base temperature. The base temperature is the temperature below which plant development stops. Researchers have shown that the accurate physiological stage of plants can be known more precisely from an accumulated heat unit rather than calendar days (Darbyshire et al., 2014; Miller et al., 2001). Indian blackberry required 1041.3 GDD for fruit development and an additional 530.9 GDD for fruit maturation when using the base temperature of 10°C (Kishore, 2019). 'Kerman' pistachio required a GDH of approximately 2500 from flowering to fruit maturity, which was calculated using a base temperature of 7°C (Zhang et al., 2021).

The objective of our study was to develop a growth model that best describes the three growth elements (shuck, shell, and embryo development) as a function of heat unit accumulation. Three pecan cultivars (Pawnee, Kanza, and Oconee) planted in five different Oklahoma microclimates were collected from fruit set until nut harvest. Commonly used nonlinear models, Logistic, and Gompertz were compared to determine the best fit model for pecan growth.

2. Materials and Method

2.1 Location and Cultivar

The study was carried out over two years in 2019 and 2020. In 2019, three cultivars of nuts were collected from five different locations. Both Pawnee and Kanza cultivars were collected from Cleveland (36°18'23''N 96°27'53''W), McMillian (34°02'08''N

96°56'25''W) and Perkins (97° 02'13''W 35°58'55''N) location. Pawnee and Oconee cultivars were collected from Idabel (33°46'06''N 94°47'39W), whereas Skiatook (36°21'37''N 96°00'27''W) had only the Pawnee cultivar. While in 2020, Pawnee and Kanza cultivar was sampled from only Perkins's location. Nuts were collected weekly in Perkins from fruit set until the harvest of the nut whereas biweekly in remaining locations. In each location, nine trees of each cultivar of same tree vigor and canopy size were selected and divided into three replications for sampling. One cluster of nuts from each direction (north, south, east, and west) of tree were collected and mixed. Ten nuts were randomly selected for further measurement. The selected nut was cut into longitudinal section and placed on a slab for measurement of area of each component (shuck, shell, and embryo). The slab was equipped with measuring tapes oriented in two directions, and a camera (Canon EOS 6D (Ota City, Tokyo, Japan)) mounted at the top for photographing with a 100 mm f/2.8 Macro USM lens.

2.2 Nut Measurements

To measure each component of nuts (shuck, shell, and embryo), Mask R-CNN (Regional Convolutional Neural Network) was used. Mask R-CNN works in two-step object detection and semantic segmentation to estimate regions. The image was divided into two stages of growth: i) small pecans (Figure 1.1a), where the embryo was not visible and, ii) big pecans (Figure 1.1b), where the embryo was visible. Each image (Figure 1.1) contained 10 nuts cut into two halves, making a total of 20 halves nut in a single picture. The object detection and segmentation model (Mask R-CNN) was developed for each stage to detect shuck and shells and embryos for the second stage. For each stage, 20 pictures were used for model training, and 20 pictures were used for the model evaluation. The model was trained using the pre-trained Resnet50 network provided by Mask I-CNN GitHub. The performance of Mask RCNN model was evaluated by two parts i) the accuracy of the object, and ii) the accuracy of the area estimation (Costa et al., 2021).

2.3 Thermal Unit

The daily temperature at each location was determined by tracking hourly temperature using data loggers (Onset HOBO® MX2300 Temperature/RH Data Loggers, Onset Computer Corporation, Bourne, Massachusetts, USA), which were installed at both the north and south direction of the trees and housed in a UV protection shield (Onset HOBO® Solar Radiation Shield, Onset Computer Corporation, Bourne, Massachusetts, USA). Growing degree hour is also called as thermal unit. Studies have shown that the use of GDH provide better estimation of heat requirement than GDD in crops like grape (Reginato et al., 2010). Furthermore, use of GDH allow the incorporation of wider range of temperature (Zhang et al., 2015) whereas the GDD only allow the maximum and minimum temperature, so GDH is used for the calculation of thermal unit in this research. The thermal units (Tu) were determined by taking a daily average and removing the base temperature threshold as shown in Eq. (1).

$$thermal\ unit = \left(\frac{\text{sum of temperature readings}}{\text{number of readings used}}\right) - 7°\text{C} \ldots\ldots\ldots\ldots\ldots\ldots\ldots\ldots\ldots\ldots\ldots\ldots (1)$$

The value of 7°C was selected as a base temperature for pecan nut growth (Costa et al., 2021; L. Zhang et al., 2021). Heat unit started to accumulate when 80% of the female flower appeared.

2.4 Models

In this study, two growing seasons (2019 and 2020) were compared with the main objective to compare the growth curve of pecan nuts at different locations. Due to circumstances, data collected in 2020 was limited to one location. Therefore, the purpose of this paper is to 1) describe the growth curve of each trait (area of shell, shuck, embryo) of pecan in 2019 after controlling the confounding effects from different locations for different cultivars; 2) model the growth curve of each trait of pecan nut over two years (2019 and 2020) for two cultivars. Gompertz and logistic models fit the standing pecan nut traits measurement taken at the different dates of the heat unit. The two models' performance was compared based on the coefficient of determination (R^2) and Akaike Information Criterion (AIC).

2.4.1 Possible growth curve

Series area of shuck, shell, and embryo from repeated measurements of pecan nuts was used at the different date of heat units. These pecan nuts were from three cultivars, five locations, and two years. The Loess method was applied to describe each pecan component's possible growth curve (Figure 1.2) of each pecan component. Statistics analysis was conducted using the ggplot package in R (R core team, 2021).

2.4.2 Growth functions

According to the smooth curves (Figure 1.2), two sigmoid growth functions were considered in the data analysis and are referred to as the Gompertz and Logistic model. The growth functions were parameterized as follows:

The Logistic model was

$$y = \frac{Asym_1}{(1+\exp((x_{mid}-tu)/scal))} \qquad (2)$$

The Gompertz model was

$$y = Asym_2 * exp(-b_2 * b_3^{tu}) \qquad (3)$$

where y represents the expected area of each trait at a given heat unit (tu), $Asym_1$ and $Asym_2$ represents the asymptote approached as the pecan nut grows, x_{mid} is the total heat units needed to reach half the asymptote, and *scal* modulates the steepness of the curve as it increases from zero toward the asymptote, b_2 translates the curve in the x-axis, and b_3 determines the growth rate.

2.4.3 Multilevel Nonlinear Mixed Models

Multilevel nonlinear mixed effect has been successfully applied to longitudinal data that involves repeated measurements within the same subject over short or long periods, which contains both fixed and random effects. For pecan nuts data, a nonlinear mixed-effects model was selected, which consider cultivar as a fixed part that indicates the response at the population level, providing a summary of how a variable change on average as a function of the thermal unit. The location or year was considered a random effect, which explained the variation in responses at the group level. This kind of model was better to account for the variation from group-level covariates (year or location). At the meantime, to reduce the measurement error, three replications were made for each cultivar at each location. The average area of each trait (shuck, shell and embryo) for cultivar and location specific was used to fit the Gompertz and logistic model.

In our study, each year or location was treated as a group-level covariate, which considers the study involving N groups drawn from a population of interest, indexed by *i*. Moreover, on the i^{th} group, n_i measurements of a continuous, univariate response y_{ij} (e.g., area of shell etc.) were observed at thermal unit $tu_{ij}, i = 1, \ldots, N$ and $j = 1, 2, \ldots, n_i$. Thus, the basic multilevel non-linear mixed-effects model was expressed in a two-stage hierarchy:

$$Stage\ 1: y_{ij} = f\left(tu_{ij}; \theta_i\right) + \varepsilon_{ij,} \qquad (4)$$

$$Stage\ 2: \theta_i = \begin{bmatrix} \theta_{1i} \\ \theta_{2i} \\ \theta_{3i} \end{bmatrix} = \begin{bmatrix} \beta_1 + \beta_4 * z_i \\ \beta_2 + \beta_5 * z_i \\ \beta_3 + \beta_6 * z_i \end{bmatrix} + \begin{bmatrix} b_{1i} \\ b_{2i} \\ b_{3i} \end{bmatrix} = \beta Z + b_i \qquad (5)$$

where $f\left(tu_{ij}; \theta_i\right)$ is a growth function of a group-specific parameter vector θ_i and a covariate vector tu_{ij}. θ_i have the same interpretation as in eqn. (2) or (3). Besides, the fixed effects, β, represent the population average of the group-specific parameters, θ_i, and the random effects, b_i, represent the deviations of the θ_i from their population average; Z is design matrices for the fixed effects, i.e. cultivars. Additionally, $\varepsilon_{ij} \sim N(0, \sigma^2)$ is an error part and $b_i \sim N(0, \Psi)$ is random effects.

3. Results

3.1 Development of shuck, shell and embryo

Through loess smooth curve, two varieties, namely Pawnee and Kanza (Figure 1.2), both showed rapid post-flowering growth in areas of shuck, shell, and embryo. The area of the component changes with the increase in heat unit. The shuck area (Figure 1.2a) of the two varieties increased the fastest between 600 and 2000 tu. The growth rate slows after 2000 tu.

The development of the shell (Figure 1.2b) was slow at the beginning, but as the thermal unit started to accumulate, shell increased in size. The rapid growth of the shell started from 600 to 2000 tu. The shell size decreased after reaching the maximum area. The embryo development (Figure 1.2c) started late for both Pawnee and Kanza cultivars compared to the development of shuck and shell. For instance, in the case of Pawnee, the development of shell and shuck started at 300 Tu. It is different from embryo development, which started from 750 tu. Pawnee showed rapid embryo growth from 800 tu, while Kanza showed rapid embryo development from 750 tu. After 2250 tu, there was a slow increase in the growth of the embryo.

3.2 Model comparison and selection for the year 2019 with a different location

Table 1.1 shows the estimations of population-level fixed effect for each cultivar in the model. In logistic nonlinear mixed model, the asymptote (β_1) approach for Kanza shell was 572.20, which is 172.17 less than Oconee shell. Besides, random group-level intercepts in each parameter of the growth function equation (2) and (3) was also estimated. In logistic the estimated variability of the σ_{Asym} parameter across locations, i.e. σ_{Asym}, was 48.07. On the other hand, the within-subject variability σ of shell were estimated as 33.22 and 42.7 from Logistic and Gompertz mixed model respectively; while for shuck and embryo, Gompertz mixed model provided a slight reduction in error variance.

Meantime, Table 1.2 displays the variance explained by the model (R^2) and Akaike's Information Criterion (AIC) for each model. For both models, the coefficient of determination R^2 was very high, ranging from 0.977 to 0.99. For shell, the AIC for Logistic mixed model was less than Gompertz mixed model; while for shuck and embryo, was opposite. Therefore, both $R^2$and AIC values indicate that logistic is the best fit for the shell region, and the gompertz model is best for embryos and shuck regions.

3.2.1 Testing the assumptions of the selected nonlinear mixed model fitted to pecan nut growth data collected in 2019 with a different location

Homogeneity of variance at subject level using residual plot (Figure 1.3) was tested and qqnorm function in R package was used to draw QQ plots as in (Figure 1.4). The scatterplots of standardized residual show the difference between observed value and the predicted value of traits among the model. The residuals were evenly around the zero line in logistic (shell), and gompertz (shuck, and embryo) which means the variance of the residuals is equal and therefore the assumption of homoscedasticity is met for these three models (Figure 1.3). The QQ plots did not show strong deviation from the provided standardized residuals indicating that the residuals are normally distributed in each selected model (Figure 1.4).

3.2.2 Predict growth curves with data collected in 2019 with different location

Figure 1.5 revealed average growth curves for three different cultivars and described the individual growth curves of cultivars at different locations. For each selected nonlinear mixed model, the individual growth curve was compared to the average growth curve fitted by the model. In the shell Logistic mixed model, the subject specific growth curve of Kanza at Cleveland is below than the population average growth curve, but the subject specific growth curve of Kanza at McMillan is above the average growth curve.

3.3 Model comparison and selection for year 2019 and 2020 with one location

Table 1.3 shows the estimations of population-level fixed effect for each cultivar in our model. For example, in logistic nonlinear mixed model, the asymptote approached for Kanza shell (β_1) is 589.32, which is 139.69 less than Pawnee shell. Besides, random group-level intercepts in each parameter of the growth function equation (2) and (3) was also estimated. For example, in the logistic nonlinear mixed model, the estimated variability of the x_{mid} parameter across years, i.e. σ_{xmid} was 26.92. On the other hand, within-subject variability σ of shell was estimated as 35.62 and 42.46 from logistic and gompertz mixed model respectively; While for embryo, gompertz mixed model provided a little reduction in error variance.

Table 1.4 shows the variance explained by the model (R^2) and Akaike's Information Criterion (AIC) for each model. For both models, the coefficient of determination R^2 is very high, ranging from 0.977 to 0.993. For shell and shuck, the AIC for logistic mixed model is less than gompertz mixed model; while for embryo, is the opposite. Therefore, both R^2 and AIC values indicates that logistic is the best fit for the shell and shuck regions, and the Gompertz model is best for embryo regions.

3.3.1 Testing the assumptions of selected nonlinear mixed model fitted to pecan nut growth data collected in the year 2019 and 2020 with one location

The residuals (Figure 1.6) were evenly around the zero line in logistic (shuck and shell), and gompertz (embryo) which means the variance of the residuals is equal and therefore the assumption of homoscedasticity is met for these three models. The QQ plots (Figure 1.7) did not show strong deviation from the provided standardized residuals line indicates that the residuals themselves are normally distributed in each selected model.

3.3.2 Predicted growth curves for year 2019 and 2020 with one location

Figure 1.8 revealed average growth curves for three different cultivars and described the individual growth curves of cultivars in different year. For each selected nonlinear mixed model, an individual growth curve was compared to the average growth curve. In the shuck Logistic mixed model, for example, the growth curve of Kanza in 2019 is higher than the population average growth curve before the water stage, and after the water stage subject specific growth curve is lower than the average growth. While the subject specific growth curve of Kanza in 2020 is lower than the population average before water stage and higher than population average after water stage.

4. Discussion

The objective of this research was to develop a model that could predict pecan nut growth stages to facilitate production decisions. The commonly used Gompertz and Logistic models were compared to select the best model that fits the pecan nut growth. The main idea behind the growth model is that calculation of thermal unit allows to establish more accurately the stage in fruits by reducing the variability observed rather than using calendar days (Salinas et al., 2019).

To predict pecan nut size growth in accordance to heat unit, the components of the nut (shuck, embryo and shell) should be measured. Measuring each component manually is time consuming and requires multiple measurement of single nuts and it neglects any deformities. But a vision-based machine learning and deep learning algorithm has been widely used in monitoring fruit and crop growth status. Pecan defect classification by using vision based machine learning methodology (Mathanker et al., 2011), fruit diameter measurement in berry by using machine vision (Qingbing et al., 2008) and defective apple detection by use of computer vision system (Zhang et al., 2015) have been developed and used successfully. Mask R-CNN (Regional Convolutional Neural Networks) combines object detection and semantic segmentation to efficiently detect objects in an image while simultaneously generating mask for each instance (He et al., 2020). For the high precision output, Mask R-CNN was used for measurement of nut components (Costa et al., 2021).

The study of development process of the plant has wide application in research which allow them to study behavior of the variables in varying situations. The study of fruit growth pattern facilitates the agriculture activities such as pre-harvest management and post-harvest management decision (Prusinkiewicz, 2004). Growth of pecan nut followed the sigmoid curve. The sigmoid fruit growth pattern is reported in different fruits like pistachio (Zhang et al., 2021), pequi (Ribeiro et al., 2018), papaya (Salinas et al., 2019), whereas double sigmoidal has been used to describe the growth of coffee berries (Fernandes et al., 2017), blueberry (Godoy et al., 2008), and peach (Pavel & DeJong, 1993). Sigmoid curves are widely used in agriculture to describe the growth model of fruit, and have generally been proven to be more suitable than linear models as they provide better adjustment and estimates of parameters with biological interpretation (Sousa et al., 2014). Logistic and Gompertz model have been used widely to describe the growth of the plant (Tjørve & Tjørve, 2017). For instance, Logistic model was suitable for growth of pear cultivars 'Shinseiki' (Ribeiro et al., 2017), longan fruits (Jesus et al., 2008), and cacao fruit development (Muniz et al., 2017) whereas Gompertz model was suitable for describing the growth of coffee seed (Sousa et al., 2014), and development of pistachio nut (Zhang et al., 2021). Because of better fit of Logistic and Gompertz model to growth and development of different fruits, these two models were selected for the pecan data fit.

In the present study, models were fitted for two datasets separately such that one compared location within a single year and the other compared years at a single location. The way to increase the reliability and efficiency of the non-linear model is to do a repeated measurement of different experimental factor to reduce the variance (Paine et al., 2012). So, the 2019 data with different locations as well as varieties was fitted separately from 2019 and 2020 data within one location. Since we have repeated measurements for each pecan nut at different times, observations are not necessarily independent of one another. Therefore, using a mixed model allows us to systematically account for population-level variability and subject-level variability. Besides, we want to estimate the growth curve for different cultivars account for the variability among a list of locations or years. "Cultivar" is fitted as a fixed effect and "Location" or "Year" as a random effect in our model. All the data set were included in training the model so that it would make conditional prediction and the cultivar variance would not contribute to the uncertainty of the prediction.

After the model is fitted, coefficient of determination is used to quantify the validity of fit. The R^2 value range from 0 to 1. Higher the value of R^2, more the variance in the data is explained by the fit. The R^2 in the Table 1.2 range from 0.975 to 0.99 and in Table 1.4 range from 0.977 to 0.9932 which is very high as compared to other fruit tree (Chuine et al., 1999; L. Zhang et al., 2021). This high R^2 reveals the high suitability of fitness to the selected model. R^2 is comparatively lower for shell and embryo as compared to shuck which could be due to sampling frequency. Since the nut exhibit the post rapid growth, biweekly sampling would be insufficient to track the growth of the nut. A more frequent sampling schedule in the nut sizing period from 750 tu to 2000 tu would facilitate to increase efficiency of model. Akaike's Information Criterion (AIC) is used to evaluate the goodness of fit. The model with the smallest AIC is selected. Based on the AIC value for 2019 with different location (Table 1.2), Gompertz is selected for development of shuck and embryo, and logistic is selected for shell. Likewise, for 2019 and 2020 data with one location, logistic is selected for development of shuck and shell whereas the Gompertz for development of embryo even though the difference was very little (Table 1.4). The Bayesian Information Criteria (BIC) is another commonly used method for model selection. But the BIC tends to select the model with few parameters and placed heavier penalty on the increase parameters (Meade et al., 2013; Wang & Liu, 2004).

The scatterplot of standardized residual against the fitted value should be distributed normally in the line of 0 of standardized residual (Figure 1.4 and 1.6). If the data are not normally distributed, then the model is not a good fit but provides heterogeneity of model. In both years fitted model, relatively less data point was observed at the mid-season which could be of less values being tested during that time. This result signifies that more sample should be collected during the rapid nut growth period to tack the growth rate (Paine et al., 2012)

Sparks (1974) classified the Pecan nut growth into four different stage i.e., lag fruit growth, rapid fruit expansion, shell hardening, and kernel growth. It is common in fruit trees; the embryo requires some time to prepare for cell division and elongation to prepare for further development. In our study, embryo growth started only after accumulation of more than 750 thermal unit starting from blooming date whereas the development of the shuck and shell started at less than 500 tu. As the nut accumulate more than 750 tu, there is the rapid fruit expansion of shuck, shell and the length of embryo period which marks the beginning of nut sizing period. The free nucleate endosperm starts to appear at the end of second week of July which force the seed coat to increase in size of embryo, shuck and shell (McKay, 1945; Thompson, 1998). Maximum expansion of ovule is observed from 1150 to 1850 tu which correspond from mid of July to mid of August (Herrera, 1990). Therefore, this period determines the final kernel dimension. Nut sizing period is also known as water stage. This stage was observed at 1000 tu at Cleveland, 1060 tu in McMillian and Skiatook, 1100 tu for Idabel Pawnee and 1220 for Oconee variety. The end of water stage is marked by the deposition of thick solidify layer of cellular endosperm known as gel stage and the shell hardening or constant growth of the shell (Dozier & Amling, 1974). Nut entered gel stage at Perkins at 1750 tu in 2019 and 1860 tu in 2020. Variation in timing of the stage from year to year is very common in orchard. This is largely determined by management practices like irrigation (Polito & Pinney, 1999). Other location recorded the gel stage at 1550 tu at Idabel, McMillian, Skiatook and Cleveland for Kanza. Whereas the Pawnee required 1664 tu in Cleveland and Oconee required 1598 tu. Interestingly, the shell size is dropped in all locations except in Idabel for Oconee variety. As the shell progress toward the maturity the lignification of the shell is completed. During this stage the development of nut size is restricted but kernel develops and continue to fill until shuck split. Fully matured pecan shell is composed of cellulose and lignin (53-71%) (Aardema et al., 2016) which provide a rigid structure. Initially, immature pecan lacks these kinds of structural elements later becomes rigid due to cell lignification. Such characteristics are important for resistance to insect (Guidone et al., 2007). For Oconee cultivar the shell and embryo continued to grow until harvest. It is generally advised to sample frequently during the rapid growth to track variation in sizes at that time period (Paine et al., 2012). Expect for Perkins, other location was sampled twice a week. So, the few sampling times would be the major reason for different shape of the shell and embryo of Oconee nut.

Dough stage also known as kernel filling stage lasts for more than one month. Late in the season when the shell growth has established, there are active oil biosynthesis which is responsible for sensory attributes (Conner & Worley, 2000). As seen in the result of smooth growth curve, Pawnee and Kanza doesn't increase in the size because of the stabilized growth of the shell. Only gradual increase is visible in size of shuck which is due to the turgidity of the shell (Worley, 1994). Management activity like irrigation is very important for maintaining the turgidity of shuck which further facilitate in shuck splitting. Shuck split is the primary indicator that determine the nut maturity. The shuck split in Pecan is due to mechanical force exerted by the lignified cell shell to the adjacent shuck (Polito & Pinney, 1999). The shuck split in the Perkins for both years recorded at 2500 tu. The shuck split is related to the shuck size (Figure 2.2a).

By using the information of growth parameters of nut based on heat unit, web applications that predict the optimal irrigation, thinning, pesticide application and harvest time can be constructed by converting the model's mathematical formulas to predict the nut component growth. The website will be customized according to site and cultivar specific data queries and to calculate predictions based on date, locations, and cultivar.

3 Conclusion

Non-linear mixed effect models-logistic and Gompertz were fitted to pecan nut growth parameters (embryo, shell, and shuck) separately for the data collected in 2019 with different location and 2019 and 2020 with one location as a function of thermal unit. With different location in 2019, Gompertz fitted best for shuck and embryo and logistic fit best for shell whereas for 2019 and 2020 with one location, Gompertz fit best for embryo and logistic for shell and shuck. The model is selected based on R^2 and AIC value. Homogeneity of the variance was checked using residual plot and QQ plot to check the assumption of fitted models. A finding from our research will help in building an integrated model with three growth parameters (shuck, shell, and embryo) which will be made publicly available through a web tool that can predict different nut development stages of nut development for multiple orchard management practices like irrigation, thinning, and pest management.

TABLE AND FIGURES

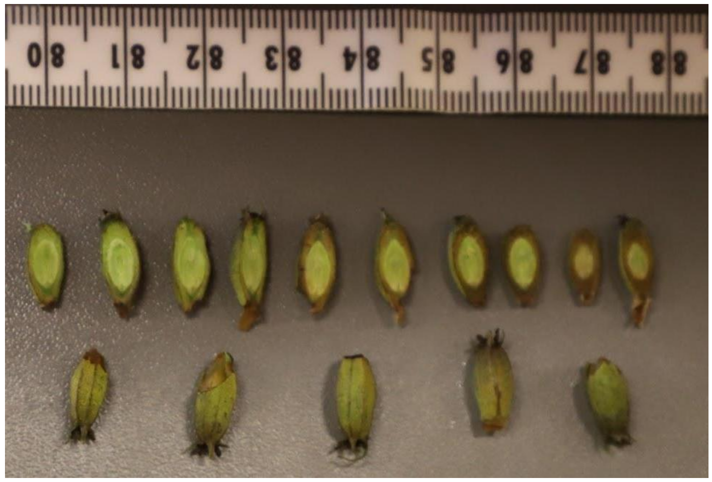

a

b

Figure 1.1. Images collected for the neural network training and evaluation. ‘Pawnee’ cultivar from Perkins location: (a) small (before beginning of water stage) and (b) big stages (beginning of water stage) (Costa et al., 2021)

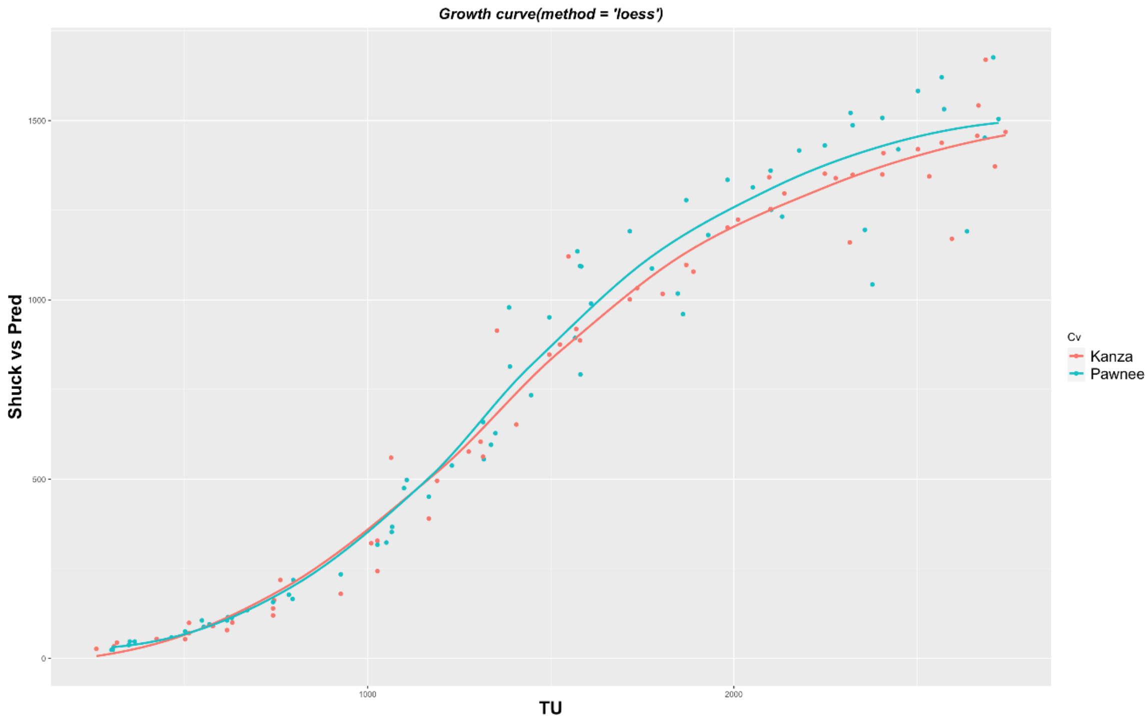
Growth curve(method = 'loess')
Shuck vs Pred
TU
0
500
1000
1500
1000
2000
Cv
Kanza
Pawnee

a

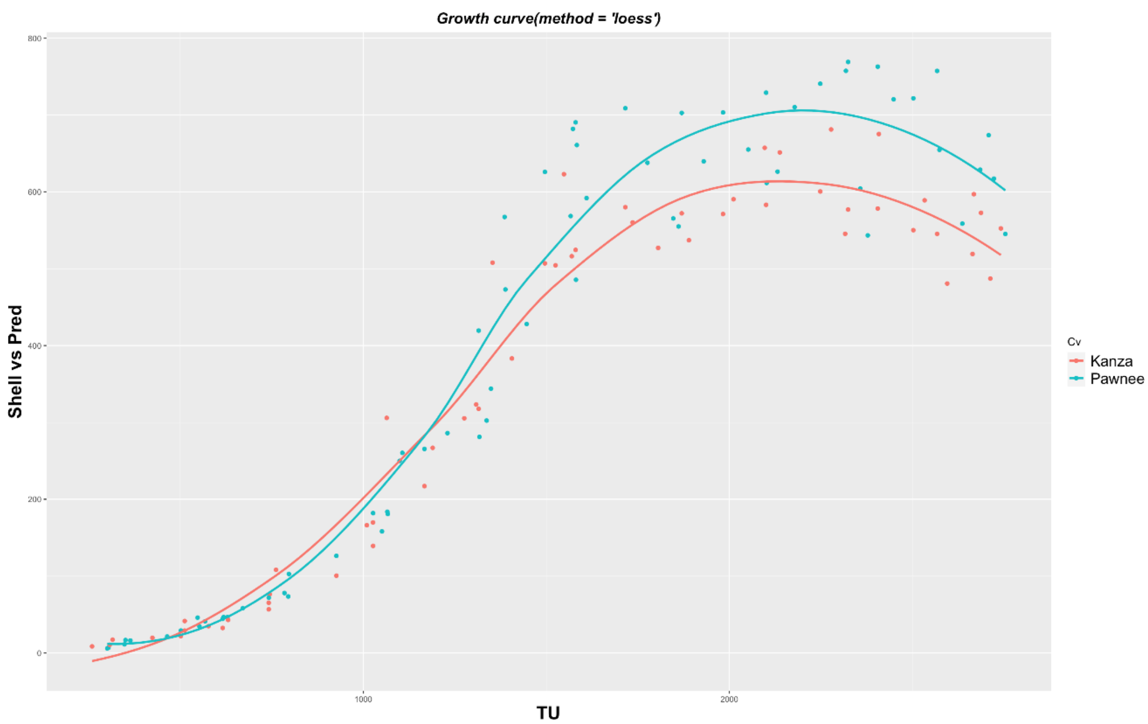
Growth curve(method = 'loess')
Shell vs Pred
TU
0
200
400
600
800
1000
2000
Cv
Kanza
Pawnee

b

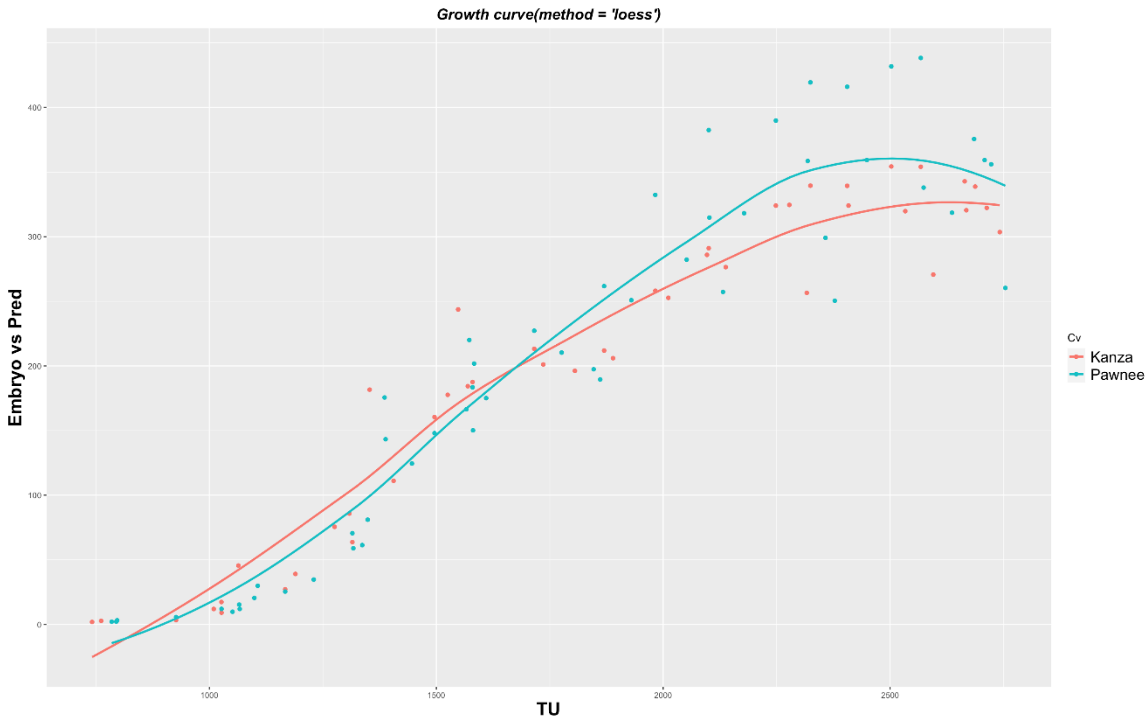

c

Figure 1.2. Growth curve of (a) shuck, (b) shell and (c) embryo development of Pawnee and Kanza cultivar of year 2019 and 2020 with year and location as a fixed effect. Red curve is for development of Kanza whereas blue is for Pawnee cultivar. The x-axis is the thermal unit (tu) calculated from bloom until harvest. The y-axis is the area of nut component (shuck, shell and embryo) in mm^2. Each dot in the graph represent the average area of the respective component of three replications for a single cultivar collected in each sampling date.

Table 1.1. Summary of fitted models and goodness-of-fit statistics for year 2019 based on data collected multiple sites in Oklahoma.

	Estimate (Std)[logistic]			**Item**	**Estimate(Std)[Gompertz]**		
	Shell	**Shuck**	**Embryo**		**Shell**	**Shuck**	**Embryo**
Fixed effect				**Fixed effect**			
$\boldsymbol{\beta_1}$	572.20(26.05) *	1335.60(86.57) *	291.31(19.91) *	$\boldsymbol{\beta_1}$	591.59(29.72) *	1514.91(102.07) *	312.57(21.45) *
$\boldsymbol{\beta_4}$**.CvKanza**	0	0	0	$\boldsymbol{\beta_4}$**.CvKanza**	0	0	0
$\boldsymbol{\beta_4}$**.CvOconee**	172.17(45.95) *	142.99(105.14)	138.90(59.21)*	$\boldsymbol{\beta_4}$**.CvOconee**	218.36(93.53)*	312.95(235.88)	226.77(122.59)
$\boldsymbol{\beta_4}$**.CvPawnee**	61.47(15.18) *	24.78(35.89)	33.79(12.93) *	$\boldsymbol{\beta_4}$**.CvPawnee**	49.0422.06) *	-75.75(54.91)	28.99(12.53) *
$\boldsymbol{\beta_2}$	1149.85(39.10) *	1302.04(47.85) *	1448.96(50.19) *	$\boldsymbol{\beta_2}$	23.31(8.45) *	6.99(0.68) *	24.58(7.11) *
$\boldsymbol{\beta_5}$**.CvKanza**	0	0	0	$\boldsymbol{\beta_5}$**.CvKanza**	0	0	0
$\boldsymbol{\beta_5}$**.CvOconee**	456.45(67.19) *	434.34(85.97) *	695.88(135.18) *	$\boldsymbol{\beta_5}$**.CvOconee**	-11.74(10.08)	-0.39(1.52)	2.36(11.93)
$\boldsymbol{\beta_5}$**.CvPawnee**	77.58(26.73) *	26.05(30.07)	115.86(40.86) *	$\boldsymbol{\beta_5}$**.CvPawnee**	47.32(31.72)	3.44(1.32) *	19.76(9.72) *
$\boldsymbol{\beta_3}$	194.03(25.49) *	314.67(22.38) *	232.14(26.73) *	$\boldsymbol{\beta_3}$	0.99(3.5E-04) *	0.99(1.20E-04) *	0.99(1.8E-04) *
$\boldsymbol{\beta_6}$**.CvKanza**	0	0	0	$\boldsymbol{\beta_6}$**.CvKanza**	0	0	0
$\boldsymbol{\beta_6}$**.CvOconee**	157.85(54.67) *	91.23(56.37)	96.97(70.99)	$\boldsymbol{\beta_6}$**.CvOconee**	0.0016(5.5E-04) *	0.0006(2.4E-04) *	0.00096(4.3E-04) *
$\boldsymbol{\beta_6}$**.CvPawnee**	-10.77(23.02)	-17.95(23.88)	2.72(34.22)	$\boldsymbol{\beta_6}$**.CvPawnee**	-0.0007(4.8E-04)	-0.0003(1.3E-04)*	-0.00019(1.8E-04)
Random Effect				**Random Effect**			
$\boldsymbol{\sigma}$ **Asym**	48.07	172.18	35.52	$\boldsymbol{\sigma}$ **Asym**	49	189.46	38.82
$\boldsymbol{\sigma}$ **xmid**	66.66	84.85	76.32	$\boldsymbol{\sigma}$ **b2**	1.07E-03	1.50E-04	6.74
$\boldsymbol{\sigma}$ **scal**	34.8	22.81	5.90E-03	$\boldsymbol{\sigma}$**b3**	2.05E-04	1.38E-04	5.60E-08
$\boldsymbol{\sigma}$	33.22	54.27	20.94	$\boldsymbol{\sigma}$	42.7	54.19	17.04
*Significant item(p<0.05)							

Table 1.2. Coefficient of determination (R-square) and Akaike's Information Criterion (AIC) for Logistic and Gompertz models to predict shuck, shell and embryo area; based on data collected in 2019 at multiple sites in Oklahoma.

Variable	Model	R-square	AIC
Shuck	**Logistic**	0.99	1068.58
Shuck	**Gompertz**	0.99	1064.84
Shell	**Logistic**	0.986	982.54
Shell	**Gompertz**	0.977	1019.91
Embryo	**Logistic**	0.975	681.93
Embryo	**Gompertz**	0.983	657.93

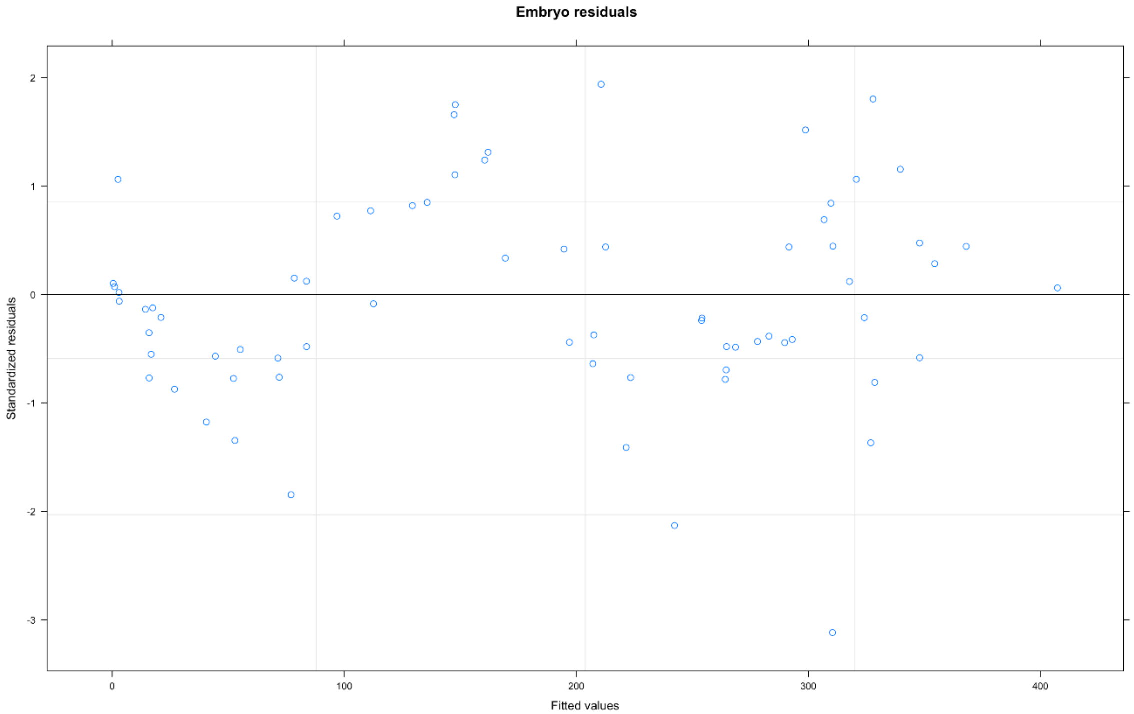
Embryo residuals
Standardized residuals
Fitted values
2
1
0
-1
-2
-3
0
100
200
300
400

a

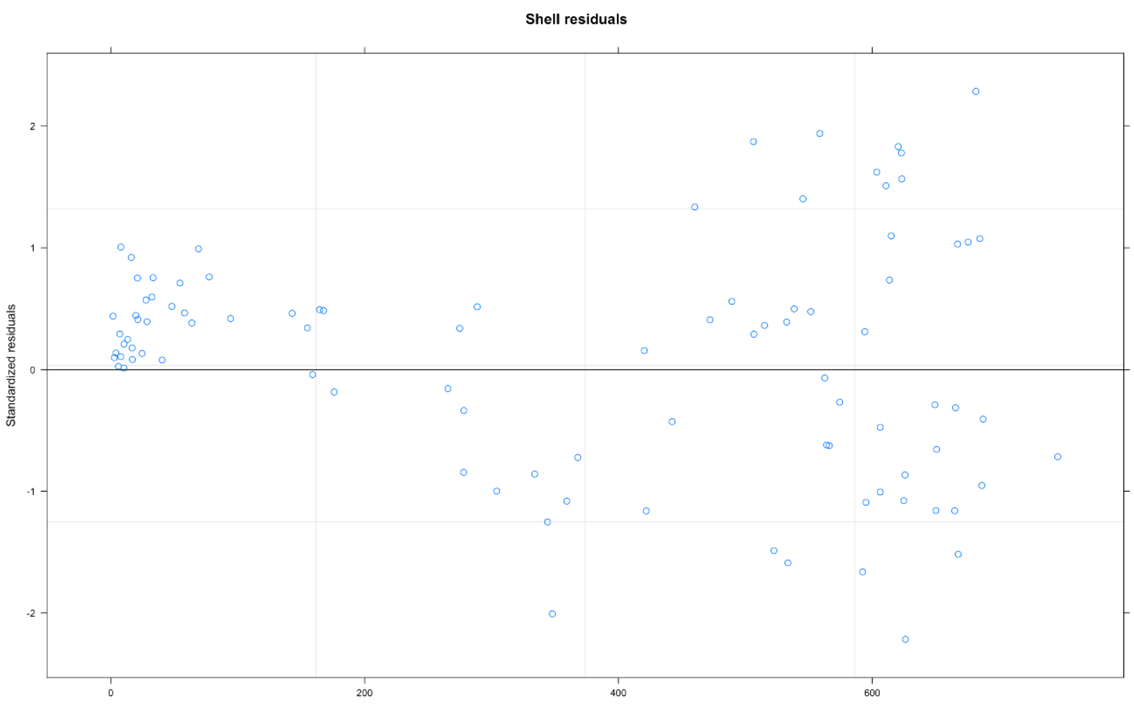
Shell residuals
Standardized residuals
Fitted values
2
1
0
-1
-2
0
200
400
600

b

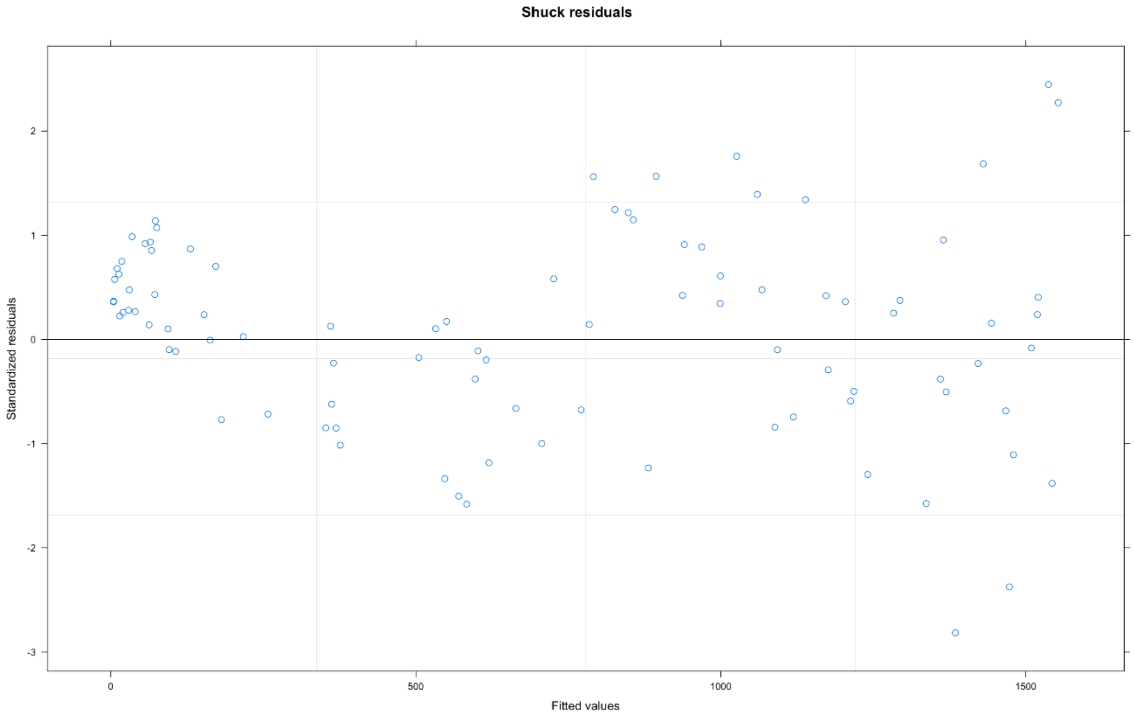

c

Figure 1.3**.** Residuals (observed - predicted) for fitted gompertz (embryo (a) and shuck (c)), and logistic (shell (b)) model fitted to pecan nut growth data collected in 2019 along with different location

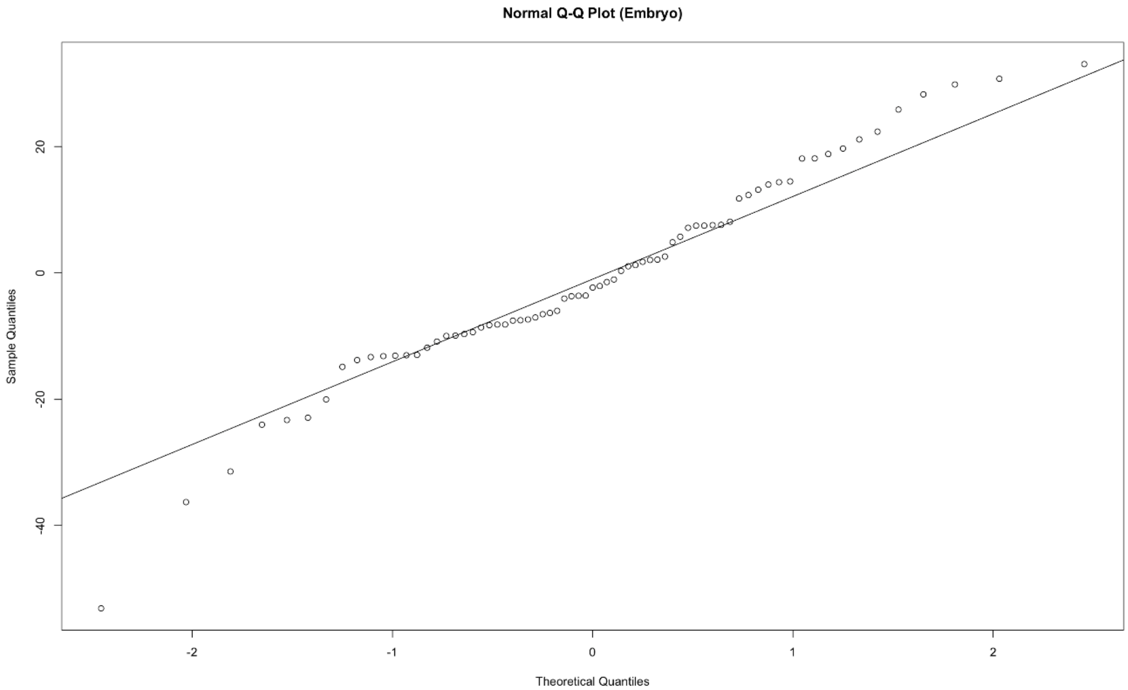
Normal Q-Q Plot (Embryo)
Sample Quantiles
Theoretical Quantiles
-40
-20
0
20
-2
-1
0
1
2

a

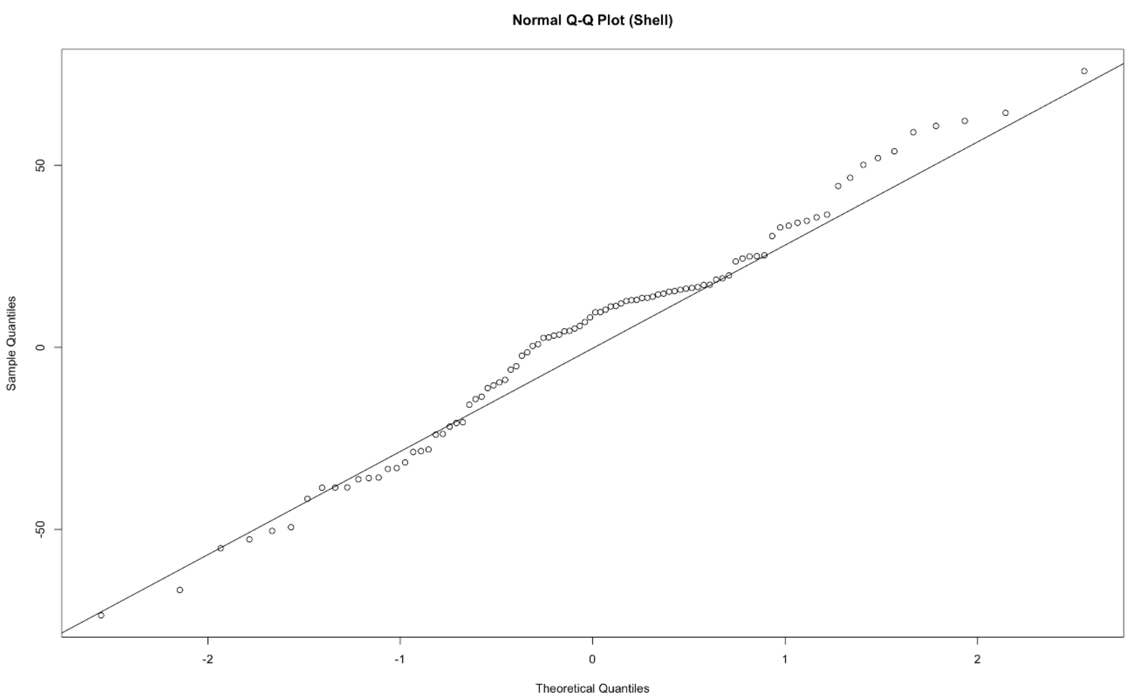
Normal Q-Q Plot (Shell)
Sample Quantiles
Theoretical Quantiles
-50
0
50
-2
-1
0
1
2

b

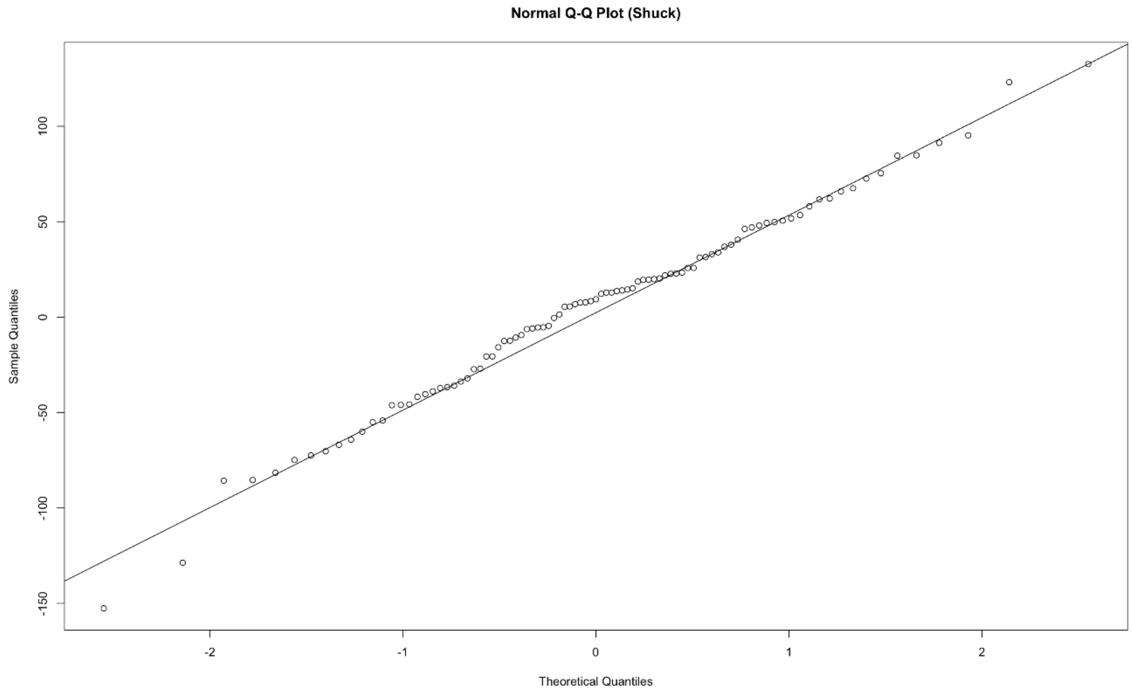

c

Figure 1.4. QQ plots for gompertz (embryo (a) and shuck (c)) and logistic (shell (b)) model fitted to pecan nut growth data collected in 2019 along with different location.

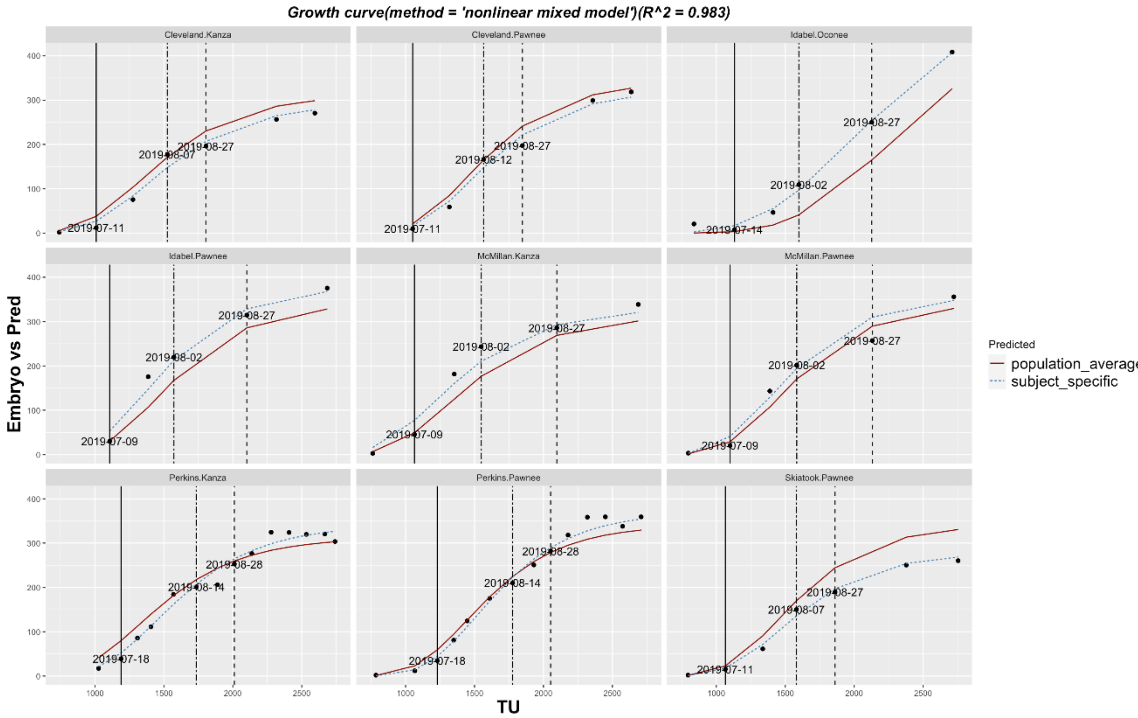
Growth curve(method = 'nonlinear mixed model')(R^2 = 0.983)
Cleveland.Kanza
Cleveland.Pawnee
Idabel.Oconee
Idabel.Pawnee
McMillan.Kanza
McMillan.Pawnee
Perkins.Kanza
Perkins.Pawnee
Skiatook.Pawnee
Embryo vs Pred
TU
Predicted
population_average
subject_specific

a

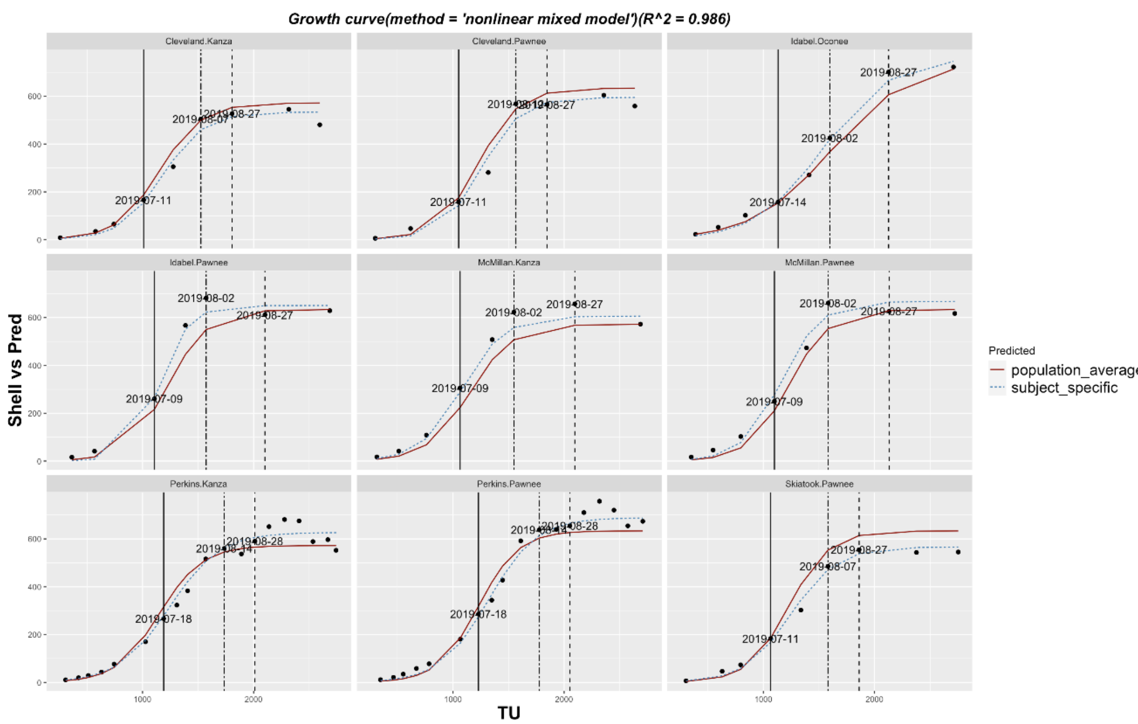
Growth curve(method = 'nonlinear mixed model')(R^2 = 0.986)
Cleveland.Kanza
Cleveland.Pawnee
Idabel.Oconee
Idabel.Pawnee
McMillan.Kanza
McMillan.Pawnee
Perkins.Kanza
Perkins.Pawnee
Skiatook.Pawnee
Shell vs Pred
TU
Predicted
population_average
subject_specific

b

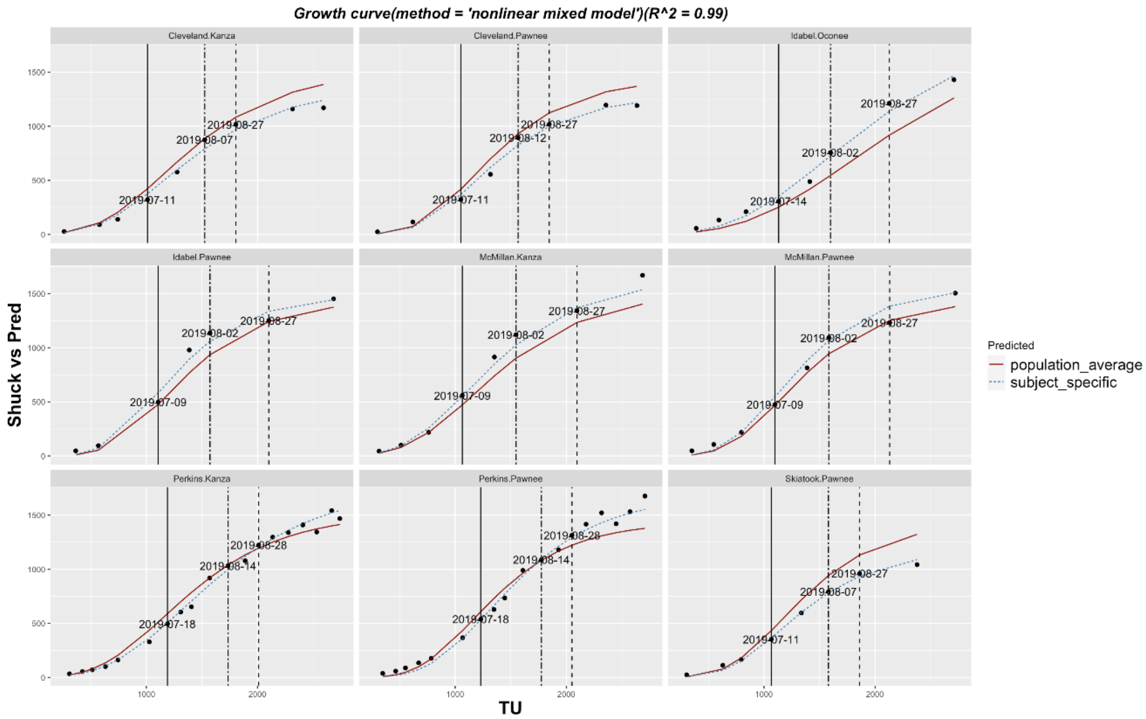

c

Figure 1.5. Non-linear mixed model for (a) embryo, (b) shell and (c) shuck with different location in year 2019. The solid line in the graph is for the beginning of water stage of nut, dot dash line is for beginning of gel stage and dashed line is for beginning of dough. The red curve represents the population average growth curve for each cultivar whereas the blue dotted curve is the subject specific growth curve for the cultivar at different locations. The two type of lines are all estimated by the same non-linear mixed effect model.

Table 1.3. Summary of fitted models and goodness-of-fit statistics for the data collected in Perkins location during 2019 and 2020

Item	Estimate(Std)[logistic]			Item	Estimate(Std)[Gompertz]		
	Shell	**Shuck**	**Embroy**		**Shell**	**Shuck**	**Embroy**
Fixed effect				**Fixed effect**			
$\boldsymbol{\beta_1}$	589.32(9.41) *	1458.32(20.34)*	342.31(9.39) *	$\boldsymbol{\beta_1}$	592.18(12.23) *	1569.83(34.71) *	353.63(21.36) *
$\boldsymbol{\beta_4}$**.CvKanza**	0	0	0	$\boldsymbol{\beta_4}$ **.CvKanza**	0	0	0
$\boldsymbol{\beta_4}$**.CvPawnee**	139.69(14.38) *	133.30(31.22) *	73.12(15.32) *	$\boldsymbol{\beta_4}$ **.CvPawnee**	157.82(20.49) *	201.53(57.40) *	73.96(18.61) *
$\boldsymbol{\beta_2}$	1240.14(28.36) *	1456.94(19.02) *	1639.54 (44.38) *	$\boldsymbol{\beta_2}$	81.66(45.31)	10.75(1.33) *	36.23(11.93) *
$\boldsymbol{\beta_5}$**.CvKanza**	0	0	0	$\boldsymbol{\beta_5}$ **.CvKanza**	0	0	0
$\boldsymbol{\beta_5}$**.CvPawnee**	40.19(26.82)	-8.05(25.33)	83.09(41.07) *	$\boldsymbol{\beta_5}$ **.CvPawnee**	-44.04(47.00)	-1.41(1.66)	15.34(20.67)
$\boldsymbol{\beta_3}$	193.89(26.53) *	323.81(17.87) *	278.29(43.64) *	$\boldsymbol{\beta_3}$	0.99(4.80E-04) *	0.99(1.10E-04) *	0.99(2.36E-04) *
$\boldsymbol{\beta_6}$**.CvKanza**	0	0	0	$\boldsymbol{\beta_6}$ **.CvKanza**	0	0	0
$\boldsymbol{\beta_6}$**.CvPawnee**	13.02(23.54)	0.12(20.65)	-11.43(34.20)	$\boldsymbol{\beta_6}$ **.CvPawnee**	0.0008(5.60E-04)	0.0001(1.50E-04)	-0.0001(3.27E-04)
Random Effect				**Random Effect**			
$\boldsymbol{\sigma}_{Asym}$				$\boldsymbol{\sigma}_{Asym}$	1.53E-03	2.09E-03	24.12
$\boldsymbol{\sigma}_{xmid}$	26.92	8.38	43.14	$\boldsymbol{\sigma}_{xmid}$	1.11E-03	1.73E-05	5.81E-04
$\boldsymbol{\sigma}_{scal}$	26.38	13.39	4.66E+01	$\boldsymbol{\sigma}_{scal}$	1.03E-04	1.43E-05	4.66E-09
$\boldsymbol{\sigma}$	35.62	45.87	20.74	$\boldsymbol{\sigma}$	42.46	46.81	17.69
	***Significant item(p<0.05)**						

Table 1.4. Coefficient of determination (R-square) and Akaike's Information Criterion (AIC) for Logistic and Gompertz models to predict shuck, shell and embryo area; based on data collected in 2019 and 2020 at Perkins location in Oklahoma.

Variable	Model	R-square	AIC
Shuck	Logistic	0.9932	807.72
Shuck	Gompertz	0.9930	811.36
Shell	Logistic	0.982	772.52
Shell	Gompertz	0.977	798.56
Embryo	Logistic	0.978	560.33
Embryo	Gompertz	0.983	541.49

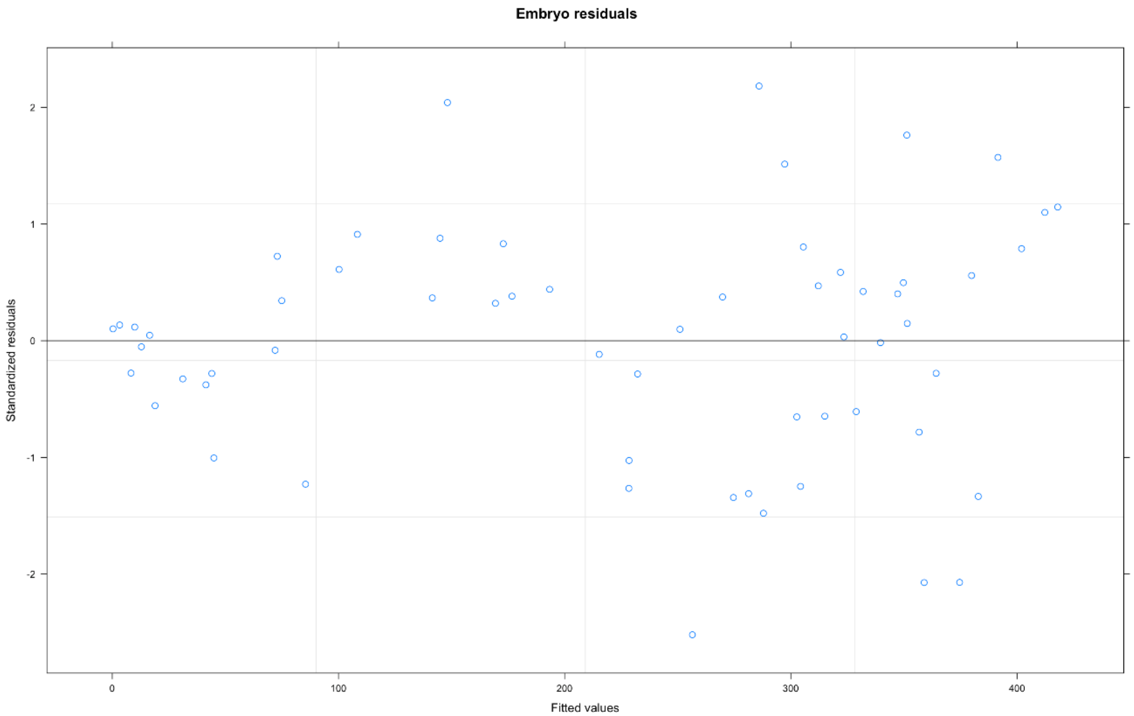
Embryo residuals
Standardized residuals
Fitted values
0
100
200
300
400
2
1
0
-1
-2

a

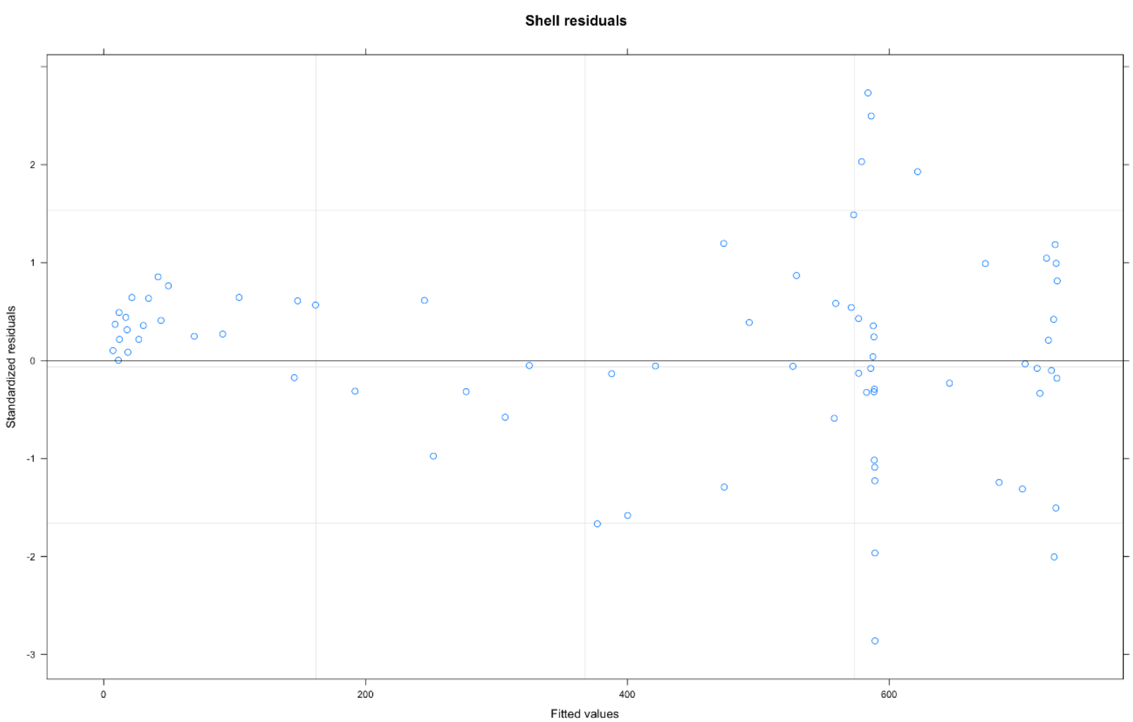
Shell residuals
Standardized residuals
Fitted values
0
200
400
600
2
1
0
-1
-2
-3

b

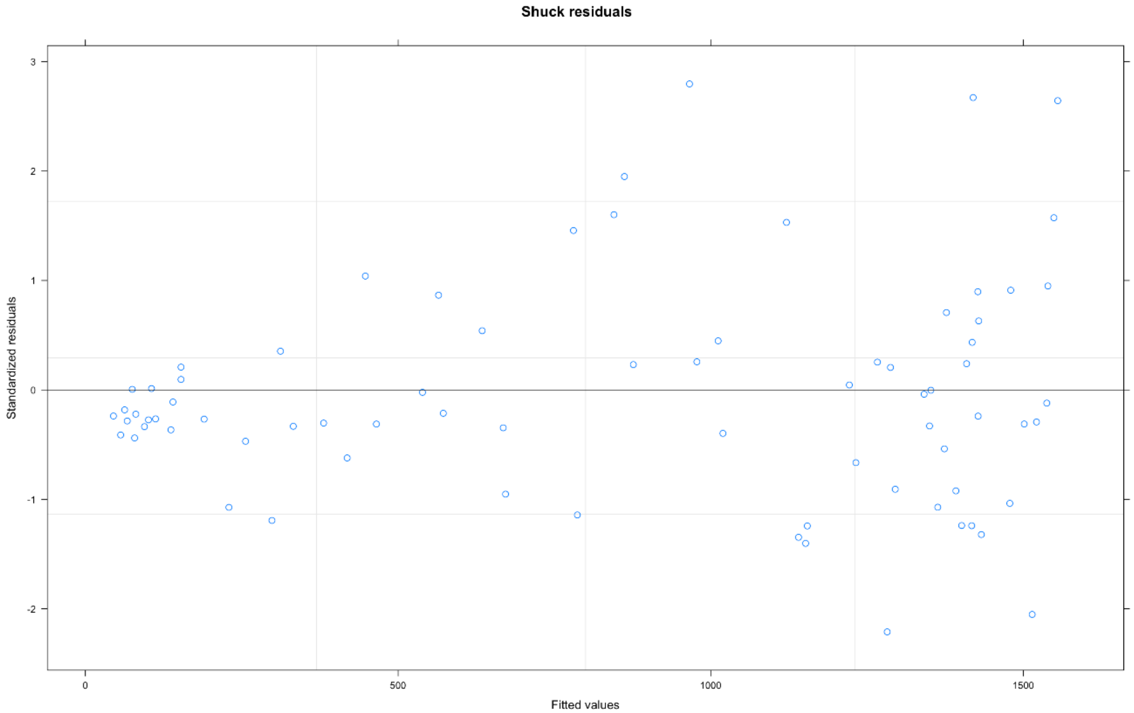

c

Figure 1.6. Residuals (observed - predicted) for gompertz (embryo (a)) and logistic (shell (b) and shuck (c)) model fitted to pecan nut growth data collected in 2019 and 2020 for one location

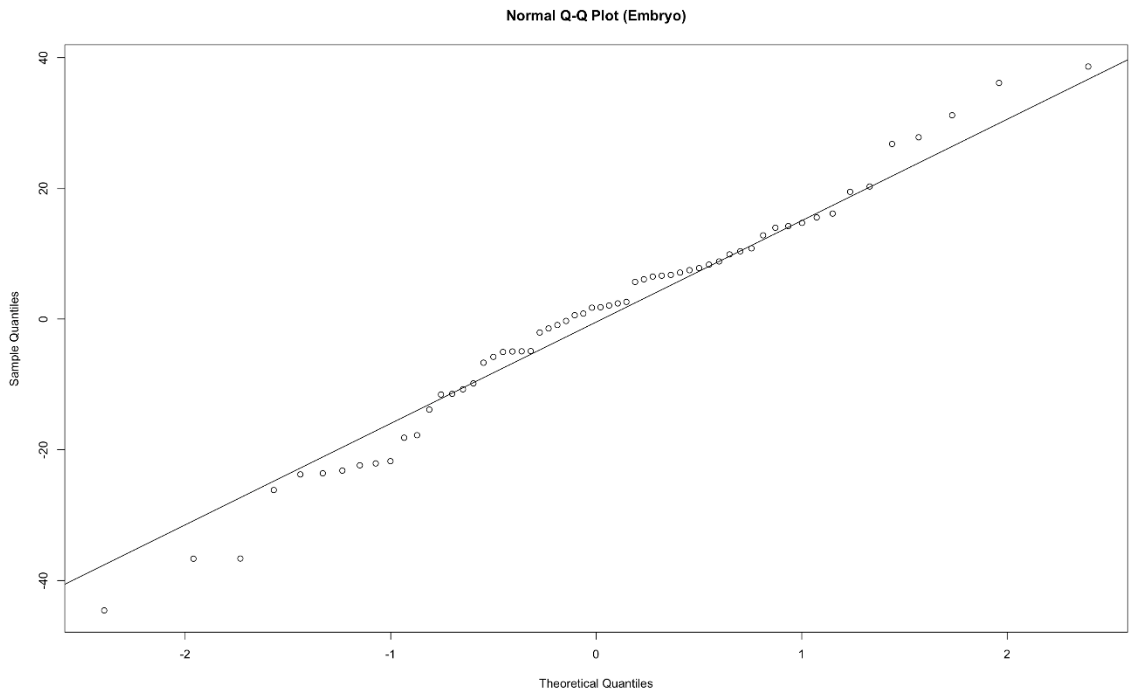
Normal Q-Q Plot (Embryo)
Sample Quantiles
Theoretical Quantiles
40
20
0
-20
-40
-2
-1
0
1
2

a

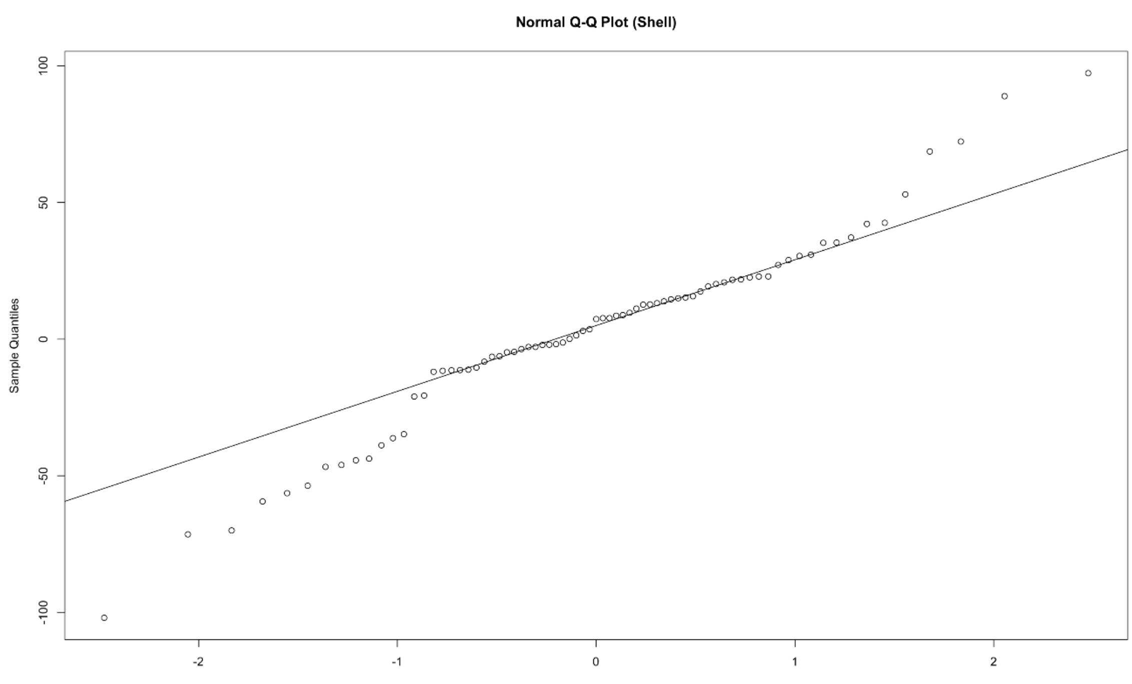
Normal Q-Q Plot (Shell)
Sample Quantiles
Theoretical Quantiles
100
50
0
-50
-100
-2
-1
0
1
2

b

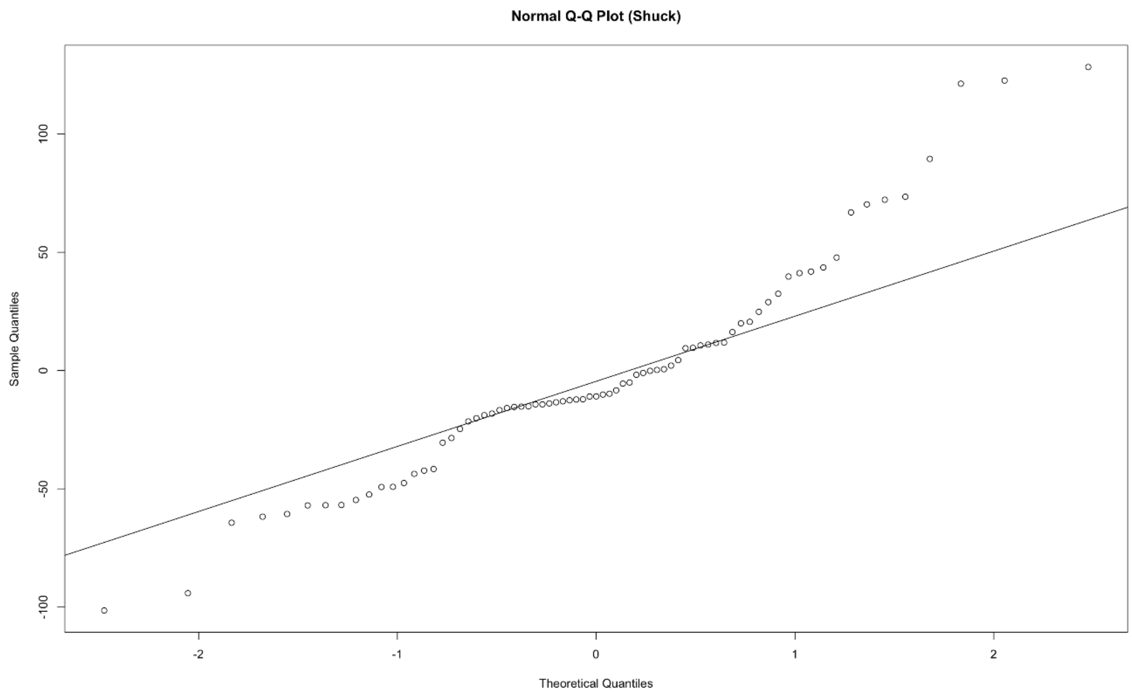

c

Figure 1.7. QQ plots for Gompertz embryo (a)) and Logistic (shell (b) and shuck (c)) model, and model fitted to pecan nut growth data collected in 2019 and 2020 for one location

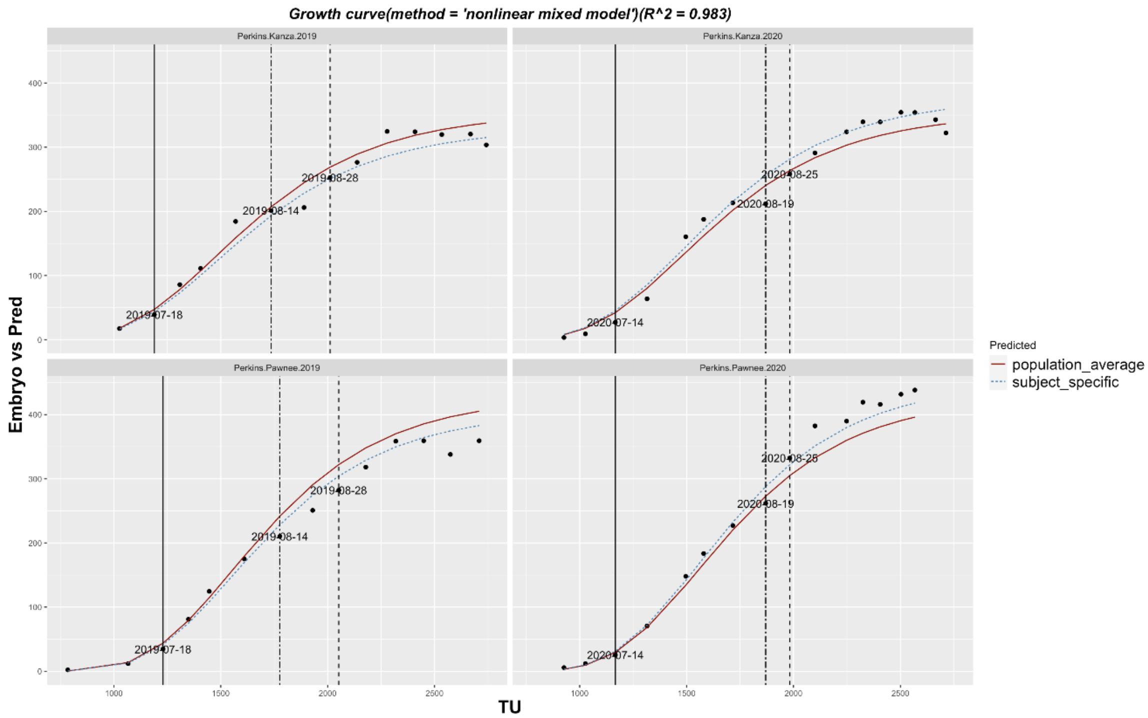
Growth curve(method = 'nonlinear mixed model')(R^2 = 0.983)
Perkins.Kanza.2019
Perkins.Kanza.2020
Perkins.Pawnee.2019
Perkins.Pawnee.2020
Embryo vs Pred
TU
Predicted
population_average
subject_specific

a

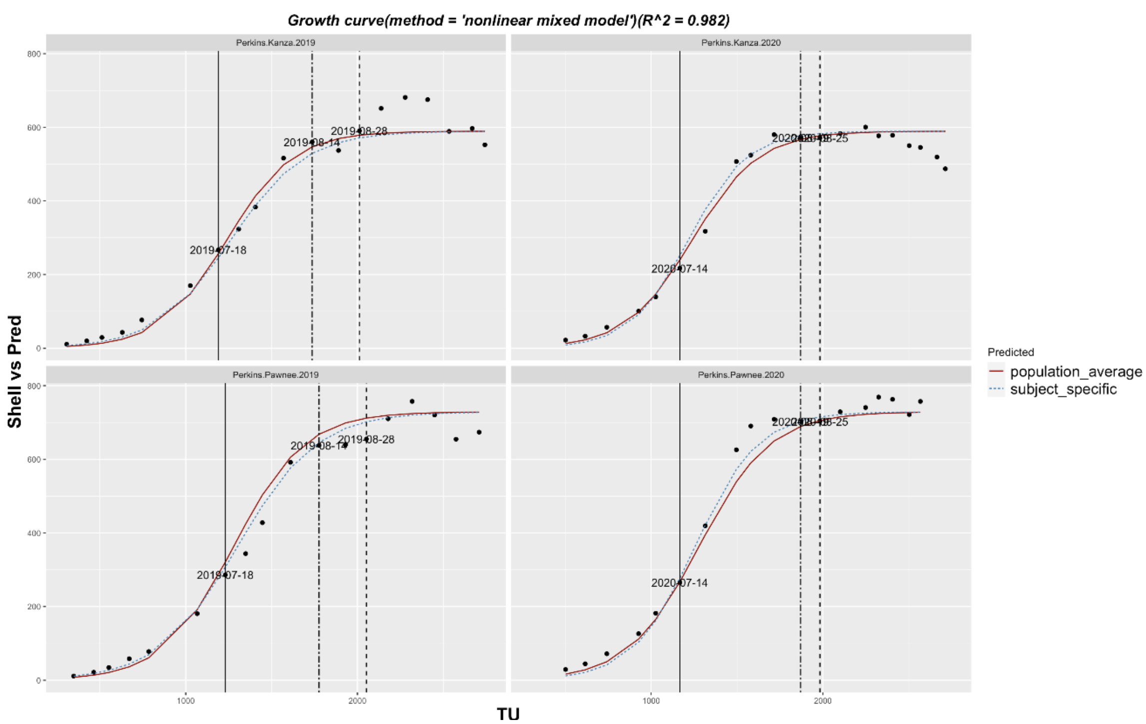
Growth curve(method = 'nonlinear mixed model')(R^2 = 0.982)
Perkins.Kanza.2019
Perkins.Kanza.2020
Perkins.Pawnee.2019
Perkins.Pawnee.2020
Shell vs Pred
TU
Predicted
population_average
subject_specific

b

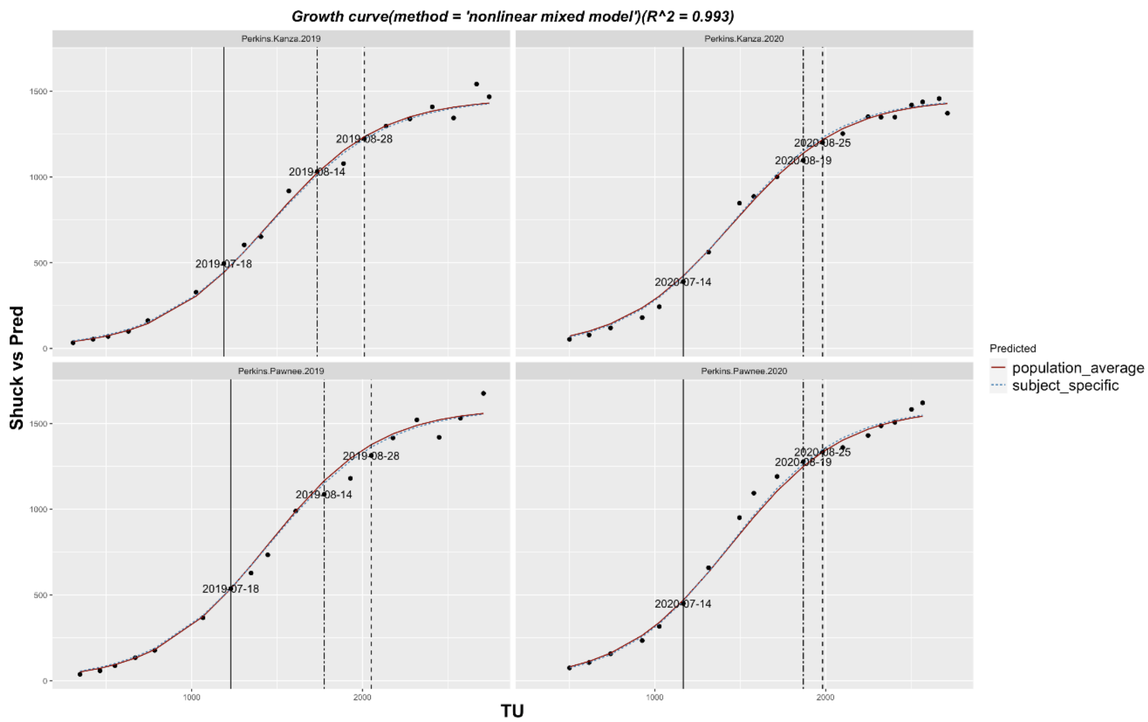

c

Figure 1.8. Non-linear mixed model for a) shuck, b) shell and c) embryo with of Perkins in year 2019 and 2020. The solid line in the graph is for the beginning of water stage of nut, dot dash line is for beginning of gel stage and dashed line is for beginning of dough. The red curve represents the population average growth curve for each cultivar whereas the blue dotted curve is the subject specific growth curve for the cultivar at different year. The two type of lines are all estimated by the same non-linear mixed effect model.

CHAPTER II

SEASONAL CARBOHYDRATE BUDGET OF PECAN DURING THE FRUITING SEASON

ABSTRACT

Pecan (*Carya illionensis* [Wangenh.] K. Koch) suffers from a very high tendency for year to year fluctuation in yield, which has a negative impact on the pecan industry. Generally, the carbohydrate budget is often suggested for irregular production in pecans. Carbohydrates are the primary source of food for trees during the different developmental stages of the fruit. Insufficient amounts of carbohydrates during the fruiting season lead to low yield or no yield, small nuts and partially filled nuts. The objective of the present study was to evaluate the seasonal carbohydrate budget by determining the nonstructural carbohydrates (NSC) especially soluble sugar and starch. A weekly analysis of sugar and starch was carried out in bark and wood of current season (Cs), first year (1-Yr) and two year (2-Yr) old shoots from fruit set until harvest of nut in year 2019 and 2020 in 'Pawnee' and 'Kanza' grown in Oklahoma. Sugar was quantified by the use of anthrone reagent method followed by micro-spectrophotometer reading of absorbance at 620 nm. The starch was determined by using a starch assay kit followed by starch quantification using the same method as soluble sugar. The sugar levels were higher in the bark as compared to the wood.

The Cs is the primary shoot that supplies food to the nut whereas the 2-Yr shoot act as backup, which participate to reserve carbohydrates for the following years. The carbohydrates were highly utilized during the kernel filling stage of the nut followed by storage of reserve in the root. The difference in carbohydrate budget in year 2019 and 2020, indicates that the role of carbohydrates is irregular production of nut. Furthermore, a low amount of starch was present throughout thousands of sample testing. This implies that the pecan tree we used are more apt to masting pattern. The amount of carbohydrates throughout the year will inform the use of pruning strategies that will increase the balanced ratio of vegetative and reproductive buds in tree.

Keywords: Pecan, carbohydrate, masting, sugar, starch

1. Introduction

Alternate bearing (one "on" year followed by "off" year) is the phenomena in which the crop doesn't bear fruit regularly, rather it has alternating years of heavy yield followed by low yield. Alternate bearing is observed in both deciduous, such as pecan, pistachio, apple, and the evergreen trees, e.g., citrus, olive, and mango (Monselise & Goldschmidt, 1982). The cycle of two or more "off" years also occurs in fruit production and such cycles are common in forest trees, known as "masting" phenomenon. Masting is an irregular and highly fluctuating sexual reproduction pattern widespread in forest trees (E. E. Goldschmidt, 2018). Masting is common in sweet chestnut, hazelnut, and elms (Gardner, 1966). E. E. Goldschmidt (2018) hypothesized that "masting and alternate bearing represent gradual steps within an evolutionary continuum, all the way through, from the wild forest tree, via the intermediary alternate and biennial bearing behavior down to the fully domesticated annually bearing fruit trees". The domestication of pecan nut (*Carya illinoiensis* [Wangenh.] K. Koch) seems to support this hypothesis (Dr. Mike Smith, pers.comm.). As compared to other tree crop, this kind of evolutionary trait is more common in pecan which are only few generations away from their wild ones and have many characteristics similar to their forebears and have retained intermediary alternate bearing—showing a more irregular character than the alternate bearing as described in other tree crops.

Carbohydrate depletion is generally accepted as a strong factor in explaining the phenomenon of alternate bearing in pecans. The severity of alternate bearing is linked mainly to three factors in pecans: 1) fruit maturity time 2) the nature of fruit growth and 3) the chemical composition of kernel (Sparks, 1974). In comparison with other fruit trees, pecan fruits mature late in the season, leaving only few days for leaves to accumulate carbohydrates for supporting flower production and fruiting the next year. The time period between fruit maturity to leaf fall in pecan is about 40 days. Additionally, dry matter in the fruit accumulates only late in the season. This allows less time for leaves to replenish their depleted carbohydrates. Pecan nuts are one of the more expensive tissues because of the large amount of oil (~70%) in its kernel. This suggests that more carbohydrates are required during the late phase of the nut growth, which results in alternate bearing of the tree.

Fruit overload can also lead to exhaustion of reserves. Depletion of nutrient reserves, carbohydrates in particular, strongly correlates with biennial fruiting cycles in mandarins *(Citrus reticulate* Blanco) (Eliezer E Goldschmidt & Golomb, 1982), pistachio (*Pistacia vera*; Rosecrance et al., 1998), pecan (Conner & Worley, 2000) and additional tree crops. This indicates that the nutrient/energy balance is the real determinant of alternate bearing.

Similarly, the conversion of vegetative buds to fruiting buds is an exhaustive process (Bustan et al., 2011). It utilizes a majority of plant carbohydrates. Massive production of flowers is not good for tree health which can result in the collapse of the tree (Paul F. Smith, 1976) or can cause a delay in carbohydrate restoration by at least one year. Rohla (2014) also demonstrated in pecans that alternate bearing is associated with the absence and abortion of pistillate flowers, and arrest in development of pistillate flowers when carbohydrates are low.

Plants are able to produce carbohydrates in presence of sunlight by using two ingredients i.e., water (absorbed by roots) and carbon dioxide (obtained by leaves) for self-sufficiency. A resource budget model (Prasad & Sakai, 2015) which is developed by researchers while studying the masting phenomenon is logical: most of the carbohydrates were used for tree growth and maintenance; development of flowering and fruiting is possible only when the amount of the carbohydrate exceeds the threshold level. In summary, crops required some time to accumulate enough energy for flowering and fruiting; it might be one or more years for entering flowering and fruiting year, characterized by large production. Thus, it is reasonable that pecan trees might have several consecutive "off" years, marked by small production.

Nonstructural carbohydrates (NSC), especially soluble sugar and starch, play a role in transport, energy metabolism, osmosis, and serving as a the building blocks for growth and structural development of the tree (Tixier et al., 2018). In almost all temperate deciduous tree species the seasonal dynamics of carbohydrates are characterized by high carbohydrate reserves in late autumn and winter, followed by depletion during spring growth, then gradually increases during the summer and early autumn (Kozlowski, 1992).

Carbohydrates are stored in an insoluble form, mainly as starch, in parenchyma cells of wood (Loescher et al., 1990; Tixier et al., 2019; Tromp, 1983) whereas the sugar is mainly present in phloem of bark tissue. Starch levels significantly decrease during the onset of bud development, which corresponds to the starch degrading enzyme activity in parenchyma cells. Thus, xylem parenchyma seems to play a pivotal role in the storage of starch and its conversion into soluble sugar and use during spring bud break (Spicer, 2014). Accumulation of soluble carbohydrates in xylem sap during the spring has been identified in many tree species, like walnut, maple, willow, and pear, and vines, such as grapes (Alves et al., 2007;Ito et al., 2012;Wong et al., 2003), indicating that the xylem plays a role in translocation of carbohydrates to promote bud break and growth.

A primary indicator of the yield of potential temperate tree is the quantity of flowers produced from floral buds (Peavey et al., 2020). Therefore, it is important to improve the distribution of flowers throughout the canopy of the tree. Pruning is one of the techniques which is used to increase light penetration in into the interior of the tree crown which influences the photosynthetic capacity of source or sink by promoting its strength (Nuzzo et al., 1999). In Oklahoma, where trees are rarely pruned, they are apt to masting or alternate bearing phenomenon, whereas in production regions where trees are mechanically pruned, constant production is recorded throughout the year. Information about storage and mobilization of temporal carbohydrates in different year-old shoot is important for cultural activities like pruning so as to maintain a balanced proportion of vegetative vs. flowering bud development so that fruit yield of the tree is constant throughout the year. Based on previous findings, we were interested in looking at the relationship between carbohydrate and fruiting capacity of the pecan. The main objective of our study was to evaluate the amount of carbohydrate budget throughout the fruiting time in the different season shoots.

2. Materials and method:

2.1. Sample collection:

The study was carried out during 2019 and 2020 at Cimarron valley research station, Perkins, Oklahoma (97° 02'13" W 35°58'55" N). Two Pecan varieties i.e., 'Pawnee' (grafted on 'Peruque' rootstock) and 'Kanza' (grafted on 'Giles' rootstock) were used. For single variety, nine trees were selected and divided into three replications. From each replication four shoots from each cardinal direction (N, S, E and W) that consists of current season (Cs), one-year-old shoot (1-Yr) and two-year-old shoot (2-Yr) were collected once per month in 2019 and once per week in 2020 (Figure 2.1). Sampling was done from fruit set until the harvest of nut. In both years and varieties different stage of nut (water, and dough) were recorded at the same time period. The water stage or ovule expansion, stage starts from mid-July to mid-August, whereas the kernel fill, or dough, stage starts from end of August. The samples were immediately placed in the ice box to reduce the heat stress and transported to the lab where each season's (Cs, 1-Yr and 2-Yr) bark (phloem) and wood (xylem) were separated and placed in the oven at 70^{o}C for 48 hours for sugar and starch quantification.

2.2.Sugar and starch quantification

By using a Mini-Bead beater 96 (Biospec Products, Bartlesville, Ok), dried wood and bark were grounded into fine and homogeneous powder. For soluble sugar, 25 mg of homogenized powder was mixed with 1 mL of ultrapure (UP) water and incubated at 70^{0}C for 15 min which was followed by centrifugation for 10 min (15,000 rpm). The supernatant was diluted by addition of UP water (1:20, v/v) and soluble sugars were measured with a glucose standard by using anthrone (0.1% (m/v) in 98% sulfuric acid) and by reading absorbance at 620nm (Leyva et al., 2008). The remaining pellet was washed twice with 95% ethanol (v/v) followed by UP water, incubated at 100^0C for 10 min to allow for starch gelatinization. Then, the pellet was allowed to cooled for 20 min in room temperature. The pellet was digested by two enzymes; 0.7 U of alpha amylase and 7 U of amyloglucosidase followed by addition of sodium acetate buffer (pH = 5.5, 0.2 M) at 37^0C for 4 hours. After complete digestion, samples were centrifuged for 5 min (15,000 RPM). The supernatant was diluted with UP water (1:4 v/v) followed by starch quantification using the same method described for soluble sugar.

2.3. Data analysis

The data were analyzed in R version 4.1.1 (R Core Team, 2021). Factors were year (2019 and 2020), season (Cs, 1-Yr, and 2-Yr), tissue (bark and wood) and variety. In one sampling time, there were three replications, two varieties, three seasons, and two tissues. From each replication, four samples were collected, one from each direction. Hence, there were a total of 144 samples per time. Samples were collected five times in 2019 and 15 times in 2020. However, the number of times were not considered for analysis of variance (ANOVA). The ANOVA was performed by using the Agricole package.

Out of 144 samples from each time, 48 samples were selected from first replication for sugar and starch analysis. The 48 samples were a combination of two varieties, two tissues, three seasons, and four directions. The graphs were generated by the use of ggplot package.

3. Result

3.1. ANOVA result

Analysis of variance was conducted as shown in table 2.1 and 2.2. There were highly significant differences in year, variety, tissue, and season ($P < 0.001$). Therefore, the data were analyzed differently for year, variety, season and tissue. Since we were interested in the main effects of variety, year, tissue and season, so the interaction effect was ignored in the table.

3.2. Soluble sugar concentration in year 2019 and 2020

In 2019, the wood sugar level for Pawnee started to decrease at slower rates from the fruiting stage and significantly at the end of August (Figure 2.2b). After the nuts were matured, the recovery rate of sugar was higher than the amount at initial stage. The same pattern was observed for Kanza wood as well (Figure 2.2f). The bark sugar for two varieties was also reduced greatly during mid-September (Figure 2.2a & e).

A clear trend of sugar pattern in different season shoot was observed in 2020. In the first week of sampling, the sugar content of both varieties increased, but as the nuts approached mid-July, the sugar decreased as shown in Figure 2.2c, d, g & h. A higher amount of sugar decreased during the end of August or the early of September in both year, variety, season, and tissue. As the nuts progress toward maturity, the sugar content of the two varieties increased. Cs, 1-Yr and 2-Yr shoot had a no difference of sugar at the start of sampling, but as the nuts progress toward development, the difference in sugar was observed in the Cs of Pawnee and Kanza during 2020 (Figure 2.2c, d, g & h). In both year and variety, the bark had a significantly higher amount of sugar content. For instance, in 2020 (Figure 2.2c), Pawnee bark had the average amount of sugar of about 50 mg/g DW (Dry Weight) at fruit set whereas the wood has 18 mg/g DW (Figure 2.2d).

3.3. Starch concentration in year 2019 and 2020

Pawnee and Kanza bark in 2019 followed a similar trend for starch content (Figure 2.3a & e). The 2-Yr old shoot had significantly higher amount of starch compared to other shoots. Likewise, the starch content for Pawnee and Kanza wood had a fluctuation trend during 2019 (Fig. 2.3b & f). The starch amount increased up to mid-September and decreased rapidly during the harvest time.

The starch amount was found to be comparatively lower than the sugar amount in both varieties for both years. For instance, Pawnee wood in 2020 (Figure 2.2d) had an average sugar content of about 18 mg/g DW at the time of fruit set whereas the starch content (Figure 2.3d) was about 8 mg/g DW. The starch amount was higher until mid-July, but after July the starch amount started to reduce (Figure 2.3c, d, g and f). After mid-September, the starch amount doubled compared to its original amount during fruit set. In both varieties the differences were observed among different shoots. The 2-Yr shoot had a higher amount of starch as compared to the other shoots. The Cs had the lowest starch content for both years in the Pawnee and Kanza varieties.

4. Discussion

The main objective of our study was to evaluate the amount of carbohydrate in the pecan shoots from fruit set until the harvest of the nuts. Knowledge and understanding of temporal accumulation of carbohydrate can be helpful in developing different cultural practices like pruning and fertilization that could promote optimal levels of carbohydrates in the trees and mitigate alternate irregular production.

In all the tests, across cultivar, year and tissue, trees showed extreme sugar exhaustion, or requirement, during the end of August or start of September, in which the tree begins the nut filling stage, also known as the dough stage. This is the stage in which the embryo of the fruit is fully developed and the oil is settled. Since most of the oil in pecan is deposited late in the season (Singanusong et al., 2003; Sparks, 1974; thor,1935), which occurs for approximately three to four weeks and depletes the carbohydrate reserves. Large exhaustion of sugar during embryo development is reported in other tree fruits, such as pistachio (Spann et al., 2008; Crane,1986), and macadamia (Cornmack & Bate 1976). In the case of peach (Da Silva et al., 2014), the carbohydrates in shoots decreased from March to June, but in November, all tissues recovered to the levels before March. For both Pawnee and Kanza, we also observed carbohydrate return (sugar and starch) in the winter season. However, the recovery levels differed between years. Taking an example of Pawnee wood (Figure 2.2b) in 2019, recovery level is about 38-70 mg/g DW during October while in 2020 (Figure 2d) recovery level is about 40 mg/g DW.

The annual carbohydrate cycle of the stem is characterized by carbohydrate depletion with each growth flush followed by carbohydrate replacement (Kim & Wetzstein, 2005). In almost all temperate deciduous tree species, carbohydrate amounts reached their maximum in late autumn and winter, to be utilized greatly during the spring as a result of the higher respiration and growth of new tissue during the season (Kozlowski, 1992). In 2019, Kanza bark (Figure 2.2e) had an average sugar content of about 80 mg/g DW during nut maturity whereas in 2020 the average sugar content (Figure 2.2g) is about 50 mg/g DW during the fruit set. We analyzed this phenomenon in two aspects; in the case of pecan anthesis, corresponding to the start of vegetative development. Thus, both the reproductive and vegetative stages are consumers of carbohydrate reserves. The lower levels of carbohydrates available at the beginning of fruit development is the result of demand caused by leaf and fruit development (Sparks, 2005) even though our result lacks the full picture of the spring carbohydrate cycle. Moreover, another budget might exist which is decided by the trees themselves: to guarantee enough carbohydrates for early fruiting, trees should have higher carbohydrates leftover after bloom.

Pecan nut development starts before the leaves have become fully functional and continues almost to the harvest. The component of nuts, i.e., shuck, shell and embryo, increase rapidly in length from July to mid-August; then the shell lignifies and the kernel starts to fill from end of August until harvest (Byford, 2005). Our result suggests that developing nuts derive their nutrients from current photosynthate and stored carbohydrate reserves. The 1-Yr and 2-Yr are the primary branches that support the current growth of the nut with a high amount of sugar, but as soon as the leaves are fully developed, the growth is further supported by the Cs (Figure 2.2b, c, d, & h) with significantly higher amounts of sugar than other season shoots.

In our results, the starch amount increased from fruit set until mid-July (Figure 2.3c, d, g, & h). During this time, the development of the fruit is slow and there is lack of photosynthate demand (Bustan et al., 2011). But after mid-July, there is rapid growth of the nut, in which sink activity is increased and the amount of starch is decreased in all year growth shoots. The fluctuation of starch in the growth stage of nuts may indicate significant involvement of starch in carbohydrate budgeting. Consequently, the sugar level also follows the same trend as starch. There is increase an increase in sugar levels until July from fruit set followed by a decreasing trend (Figure 2c, d, g, & h) until the kernel fill stage of the nut. This result aligns with the findings which showed that the shoot carbohydrates decrease during the liquid stage of ovule development (Wood & McMeans, 1981).

In both varieties, i.e., Pawnee and Kanza (Figure 2.3), the starch concentration throughout the season is greater in 2-Yr followed by 1-Yr and lowest in Cs. Starch is mainly stored in the wood parenchyma cells (Tixier et al., 2019).Two-Yr old shoots had high starch content compared to other shoots throughout the season. The starch concentration increased greatly after the kernel fill stage in the nut. The increase in starch is for storage for the dormancy period in the root. The starch amount was less than 10 mg/g DW during the fruit set in the years 2019 and 2020. Low levels of starch throughout the fruiting season coincide with an increase in the amount of soluble sugar for possible remobilization of the carbohydrates (Nzima et al., 1997).

Our observation showed the sugar level in the current year's section was higher than the other sections, especially in 'Pawnee' (Figure 2.2c & d), but more starch was stored in two-year-old shoots (Figure 2.2e & f). This result created a vivid image of the functions of different sections in the shoot. The current shoot, which bears fruits, continuously receives supply of carbohydrates from leaves is the sugar station and provides "food" to the developing fruits (Nzima et al., 1997) whereas, the older shoots act as reservoir of carbohydrates for the following years. However, it is hard to understand the distance of the carbohydrate's translocation from two older shoot to the current year shoot and vice versa.

In tree fruit which tends to have alternate bearing pattern, the CHO reserves at the end of the “on” year is low whereas the carbohydrate reserves at the end of an “off” year tends to be higher (Monselise & Goldschmidt, 1982). During 2019, Pawnee wood (Figure 2.2b) has a recovery of more than 55 mg/g DW. Whereas in 2020, recovery is about 40mg/g DW even though we don’t have the carbohydrate storage in the root during winter. The same pattern is observed for the Kanza wood (Figure 2.2f & h). The difference between the carbohydrate budget pattern in 2019 and 2020 gives us a clue toward understanding masting and alternate bearing phenomena due to carbohydrate differences. Carbohydrate accumulation doesn’t follow a yearly cycle. In other words, carbohydrate budgeting in a multi-year cycle indicates that carbohydrates could drive the masting or biennial fruiting pattern. We also hypothesize due to high amount of resource budget in 2019, led to more fruit production followed by large exhaustion of sugar during 2020 which led to less sugar recovery.

Carbohydrate mass fractions tend to be higher in bark tissues (Kozlowski, 1992). The bark, in agreement with reports of olive species, had less starch but significant amounts of soluble sugars due to its function as a sugar-conducting tissue (Bustan et al., 2011). Higher amounts of sugar in bark compared to wood might be related to bidirectional flow of photosynthate from leaves (Davis & Sparks, 1974).

Another interesting finding is that through thousands of samples testing, lower starch levels appeared in pecan trees. The starch level in pecan was approximately two to three times lower than starch of pistachio and walnut (Nzima et al., 1997; Tixier et al., 2017). As we know, pistachio tightly follows an alternate bearing pattern, and the pecan trees we used are more apt to the masting pattern. There could be a cycle that takes more than two years in pecans that is driven by lower starch or the mechanically pruned trees that follow alternate bearing might have a higher level of starch than the rarely pruned.

5. Conclusion

The soluble sugar and starch were quantified for two varieties i.e., Pawnee and Kanza for two years. The result showed that there is extreme sugar exhaustion during the kernel fill stage of the tree. The Cs shoot is the primary branch that supplies carbohydrates to the nuts whereas the second-year branch acts as a backup. Higher amount of carbohydrates during early autumn and reduced amounts following the spring season could be due to large amount of carbohydrate utilized for spring flush. Also, the difference in carbohydrate budget pattern between two year gives us a clue that pecan as alternate or masting tree. Moreover, the low amount of starch in wood throughout thousands of samples testing gives a clue that pecan likely has a masting pattern. This information will guide different management practices, such as pruning and fertilization, that could promote optimal carbohydrate in tree.

TABLE AND FIGURES

Figure 2.1. Brach showing each section; Current season (Cs), one-year old (1-Yr) and two-year old (2-Yr)

Table 2.1. ANOVA for sugar concentration for year 2019 and 2020 for variety Pawnee and Kanza in bark and wood tissue for three different seasons (Cs, 1-Yr, and 2-Yr).

	P-value
Season	<0.001
Variety	<0.001
Tissue	<0.001
Year	<0.001

* Significant at the 0.05 probability level; ** significant at the 0.01 probability level; *** significant at the 0.001 probability level; NS not significant

Table 2.2. ANOVA for starch concentration for year 2019 and 2020 for variety Pawnee and Kanza in bark and wood tissue for three different seasons (Cs, 1-Yr, and 2-Yr)

	P-value
Season	<0.001
Variety	<0.001
Tissue	<0.001
Year	<0.001

* Significant at the 0.05 probability level; ** significant at the 0.01 probability level; *** significant at the 0.001 probability level; NS not significant

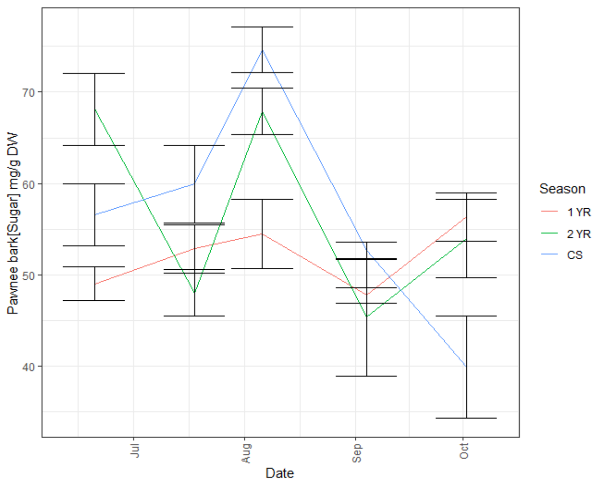
Pawnee bark[Sugar] mg/g DW
70
60
50
40
Jul
Aug
Sep
Oct
Date
Season
1 YR
2 YR
CS

a

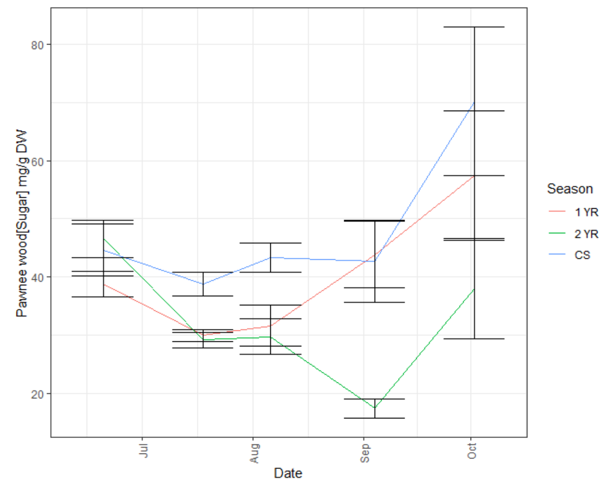
Pawnee wood[Sugar] mg/g DW
80
60
40
20
Jul
Aug
Sep
Oct
Date
Season
1 YR
2 YR
CS

b

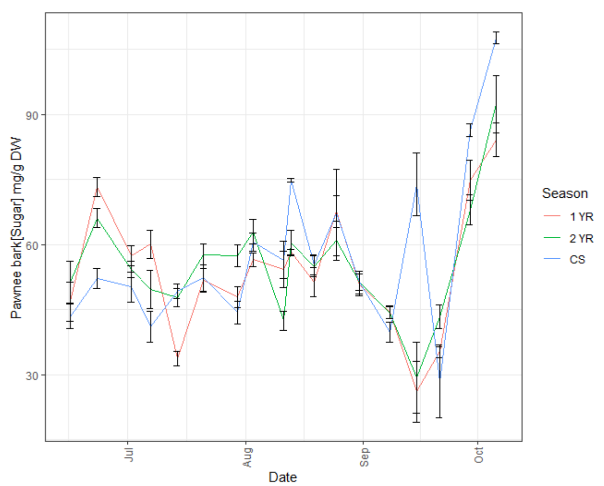
Pawnee bark[Sugar] mg/g DW
90
60
30
Jul
Aug
Sep
Oct
Date
Season
1 YR
2 YR
CS

c

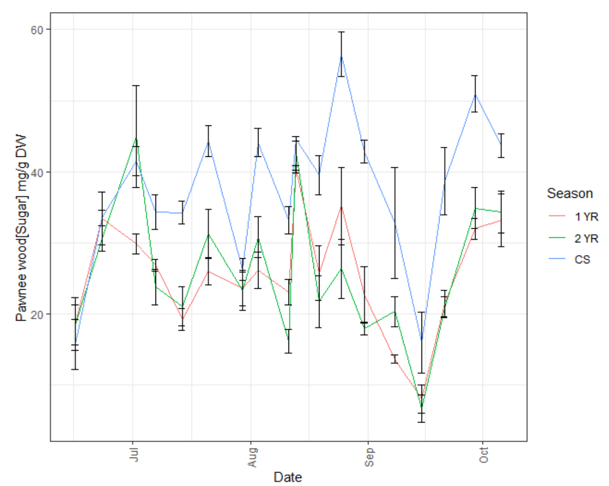
Pawnee wood[Sugar] mg/g DW
60
40
20
Jul
Aug
Sep
Oct
Date
Season
1 YR
2 YR
CS

d

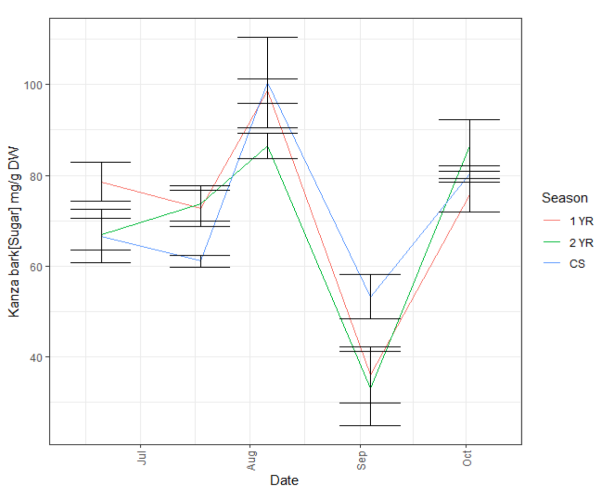
Kanza bark[Sugar] mg/g DW
100
80
60
40
Jul
Aug
Sep
Oct
Date
Season
1 YR
2 YR
CS

e

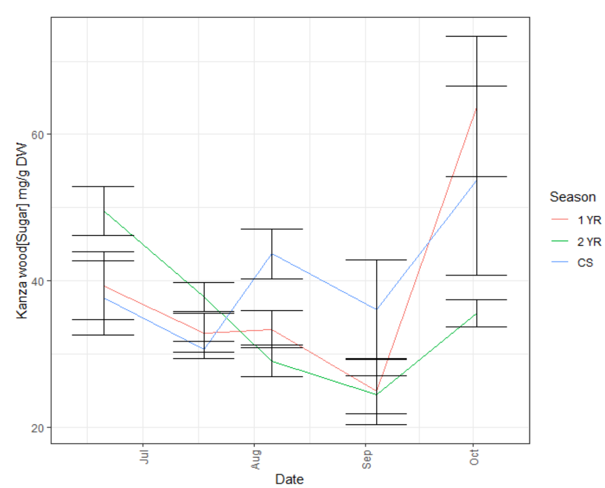
Kanza wood[Sugar] mg/g DW
60
40
20
Jul
Aug
Sep
Oct
Date
Season
1 YR
2 YR
CS

f

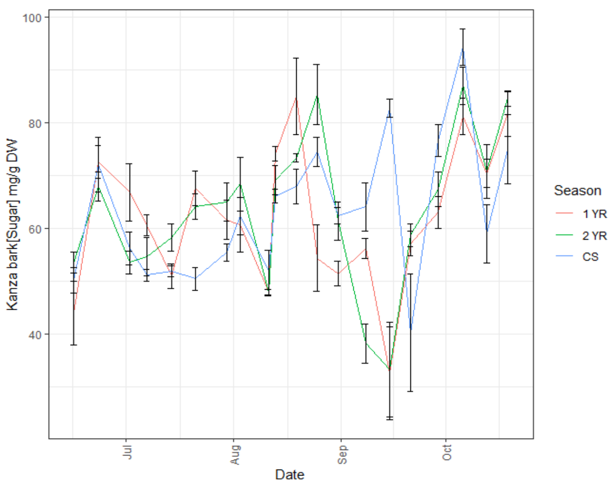

g

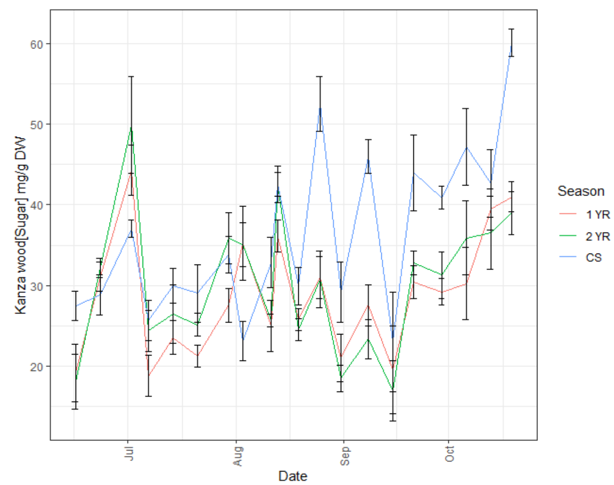

h

Figure 2.2. Average sugar content (±Standard error) in Pawnee and Kanza bark during 2019 and 2020 a) Pawnee bark 2019, b) Pawnee wood 2019, c) Pawnee bark 2020, d) Pawnee wood 2020, e) Kanza bark 2019, f) Kanza wood 2019, g) Kanza bark 2020, and h) Kanza wood 2020. Different line in the graph is for the different season shoot i.e., blue is for Cs (Current season), red is for 1-Yr (one-year-old) and green is for 2-Yr (two-year-old) shoot.

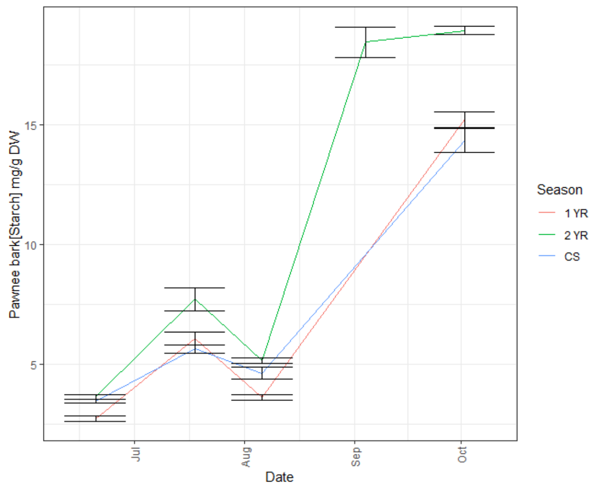
Pawnee bark[Starch] mg/g DW
Date
Jul
Aug
Sep
Oct
Season
1 YR
2 YR
CS

a

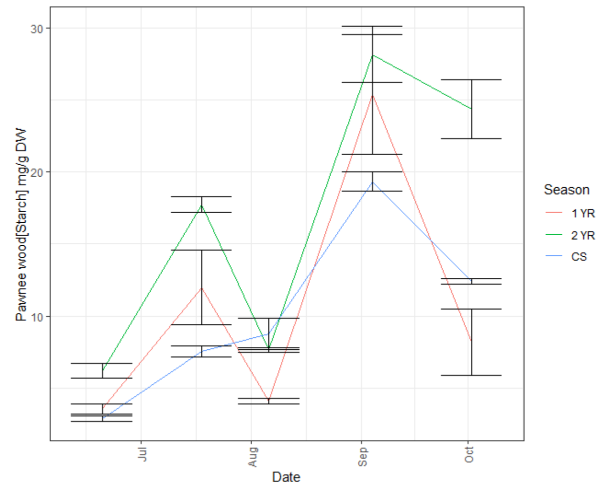
Pawnee wood[Starch] mg/g DW
Date
Jul
Aug
Sep
Oct
Season
1 YR
2 YR
CS

b

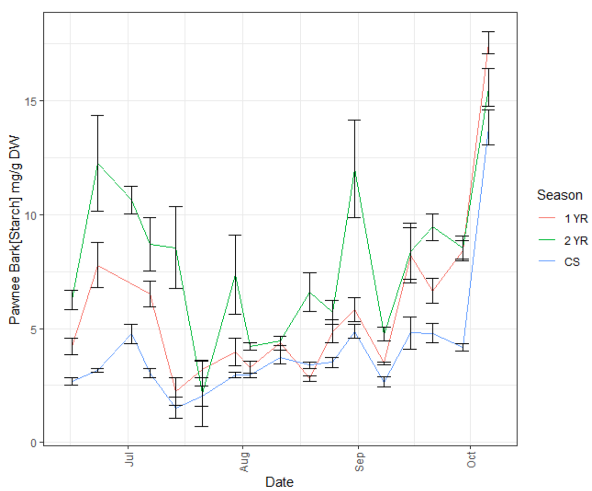
Pawnee Bark[Starch] mg/g DW
Date
Jul
Aug
Sep
Oct
Season
1 YR
2 YR
CS

c

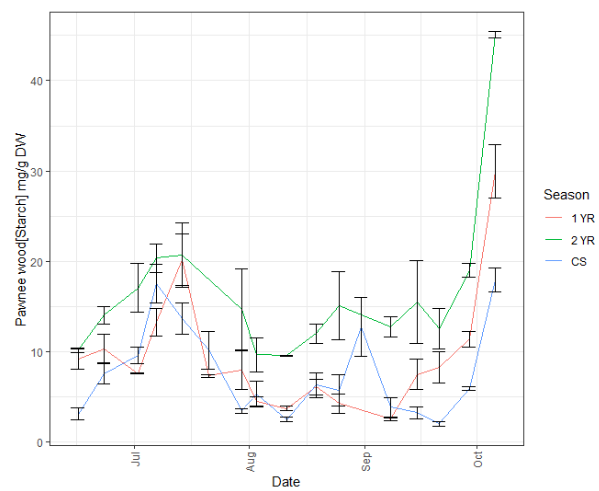
Pawnee wood[Starch] mg/g DW
Date
Jul
Aug
Sep
Oct
Season
1 YR
2 YR
CS

d

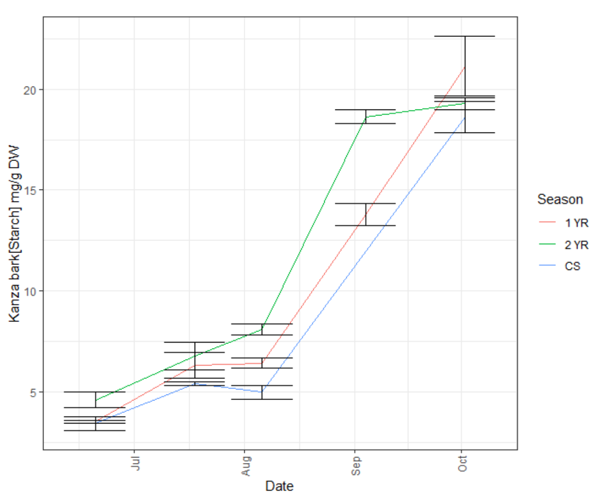
Kanza bark[Starch] mg/g DW
Date
Jul
Aug
Sep
Oct
Season
1 YR
2 YR
CS

e

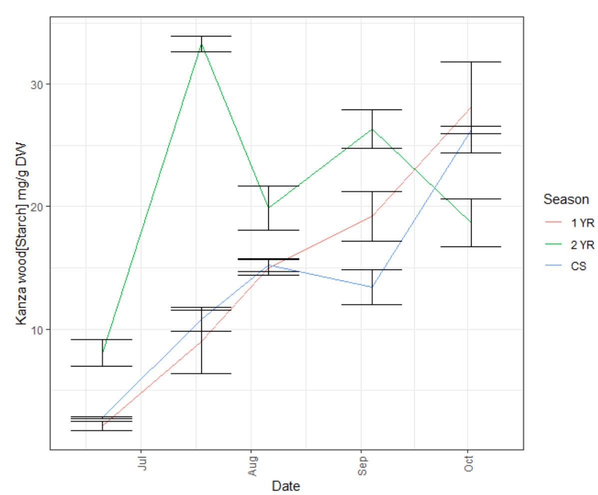
Kanza wood[Starch] mg/g DW
Date
Jul
Aug
Sep
Oct
Season
1 YR
2 YR
CS

f

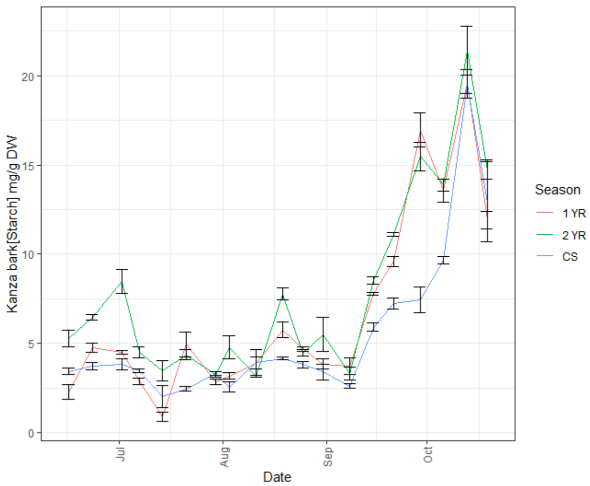

g

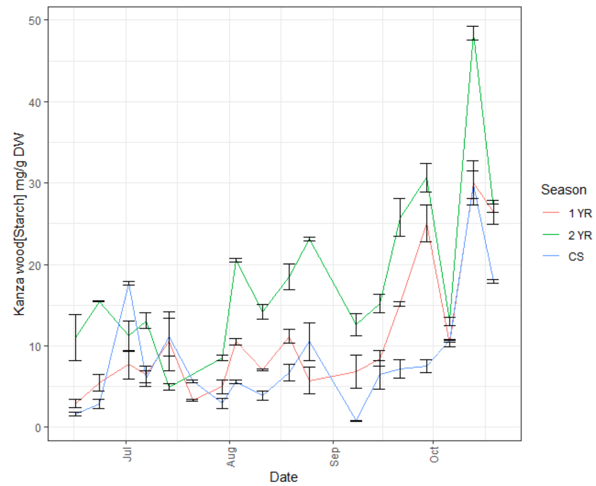

h

Figure 2.3. Average starch content (±Standard error) in Pawnee and Kanza bark during 2019 and 2020 a) Pawnee bark 2019, b) Pawnee wood 2019, c) Pawnee bark 2020, d) Pawnee wood 2020, e) Kanza bark 2019, f) Kanza wood 2019, g) Kanza bark 2020, and h) Kanza wood 2020. Different line in the graph is for the different season shoot i.e., blue is for Cs (current season), red is for 1-Yr (one-year-old) and green is for 2-Yr (two-year-old) shoot.

CHAPTER III

IRRIGATION AND WEEVIL MANAGEMENT: DEVELOPING PRACTICAL APPLICATIONS BASED ON THE PECAN NUT GROWTH MODEL

ABSTRACT

Oklahoma is one of the largest producers of pecan (*Carya illinoiensis* [Wangenh.] K. Koch) with a production of approximately 305 million pounds of nuts in 2020. Often the growers in Oklahoma experience a severe fluctuation of nut production coupled with large amount of water demand during summer and a high infestation of insect pests at the time of harvest. The water stage is the important stage of the nut where irrigation determine the length of the embryo. Similarly, the shell hardening is another important stage where the management of the weevil is crucial. From preliminary research during 2019, we found that orchards in Perkins, Oklahoma is irrigated more than is necessary. This research was conducted to find out whether the nut can thrive in minimum irrigation. Two varieties (Pawnee and Kanza) were selected, and for a single variety, there are three treatments: full-irrigation (regular rate), half-irrigation (half of the regular rate), and no-irrigation. This research concludes that the some of the varieties can withstand a reduced amount of irrigation, like Pawnee. The quality of the nut appeared higher in the Pawnee variety with full irrigation whereas in Kanza such quality did not occur. This implies that irrigation alone is not the indicator of the quality of nut rather it also depends upon the varieties. On

another hand, shell hardening is the defense mechanisms against the pecan weevil. To know whether the shell hardening restricts the weevil oviposition, six Kanza nuts infested with weevil were divided into 12 section. In each section the hardness was measured. The result signifies that the weevil oviposit in those sections which have a low hardness value and this low value is present in the suture line signifying that suture is the weakest point. On the other hand, the hardness tested on the Pawnee and Kanza nut showed that the Kanza nut have a high firmness compared to the Pawnee nut. This information can be useful for breeders to increase tolerance or avoidance of the pests.

Keywords: Hardening, water, irrigation, suture, quality

1. Introduction

From our nut growth model (Chapter 1), we found that the nut's rapid growth occurs in the water stage. The water stage is the important stage of the nut in which the liquid endosperm is present in the developing nut (Figure 3.1) (Carroll et al., 2015; Sparks, 1995). Endosperm is the tissue which will provide nutrients for the development of the kernel. This stage generally starts from mid-July to mid-August depending upon the cultivar and growing location. During the water stage, trees require a large amount of water. Drought stress during water stage results in increasing of fruit drop, as well as poor kernel filling (Sparks, 1995). During the summer month, pecan trees required 8 inches of water in Oklahoma (Upson et al., 2012). However, in Oklahoma which is mostly occupied with native trees, generally minimal irrigation systems are practiced due to expenses associated with the installation of irrigation systems. Meanwhile, some growers are overwatering their trees which results in a "water split" of nut during water stage (Thompson, 1998). Preliminary research conducted at the Cimarron Valley Research Station, Perkins, Oklahoma by installing WATERMARKER indicated that the pecans are irrigated more than necessary (Figure 3.2) (Zhang et al., 2021). There is a question to consider: could nuts thrive in minimal irrigation? The purpose of this study is to compare different kinds of irrigation reduction with currently recommended watering schedule using mid-day stem water potential measured by pressure chamber.

The water potential (ψ; units MPa) is a simple indicator of water status of leaves; lower water potential means the tree has difficulty in dragging the water from roots and signify that the tree needs to be watered. About 97% of water in the plant is used for transpiration whereas 3% of the water is used for metabolic function of the tree (Sinha, 2004). Transpiration in the leaves is the force which drags water from the root to the leaf and causes negative pressure inside the xylem (Vesala et al., 2017). Measuring the water potential by the use of a pressure chamber is a common and direct method for evaluating the water status of fruit trees like in peach and plum (Garnier & Berger, 1985; McCutchan & Shackel, 1992). Hence, water status of the tree can be detected by measuring water potential (ψ) in leaves, as well as stem. A plant-based measurement such as ψ is best for scheduling the irrigation as it integrates the condition of plant, soil and atmospheric condition (Wells, 2015).

On the other hand, from the nut growth model (Chapter 1), stable growth of the nut is visible as soon as the water stage ends. The end of the water stage is marked by the beginning of shell hardening (Herrera, 1990). Shell hardening is the defense mechanism developed by the nut to protect itself from insect pests and to prevent moisture loss (Daane et al., 2016). In pistachio, shell hardening provides growers important information for controlling insects, such as mirid (Calocoris norvegicus) and lygus bugs (Lygus hesperus), which can injure the young nuts before reaching the hardness value where pesticide application is not obligatory (Daane et al., 2016). Pecan weevil (Curculio caryae) is one of the major insect pests in pecan orchard which results in fluctuation of nuts production (Mulder et al., 2012). Pecan weevil can cause three types of seasonal damage in nuts: early season damage; which occurs at the water stage where weevils puncture the young nut resulting in nut falling from the tree, late season damage; occurs when the nut are matured, female weevils lay eggs by causing ovipositional damage and final damage is caused by feeding of larvae on the kernel as a result of hatching of egg (Mulder et al., 2012). Management of the weevils is very important in orchards. In the case of hazelnut, it is advised to select strongly hardened nuts because it is generally considered that the higher the hardness or firmness of the nut, the greater the difficulty in penetrating the shell by the weevil (Guidone et al., 2007). The relationship between weevils and the shell hardening has been poorly studied in pecan. Hence, the present research was carried out to find out how shell hardness restricts the weevil oviposition. Furthermore, we hypothesized that the weevil activity is restricted by increased shell hardness.

This project was hence carried out with two objectives as follows:

1. To find whether the nut growth at water stage can thrive minimal irrigation using mid-day stem water ψ measured by pressure chamber.

2. To find out if weevil oviposition behavior is affected by shell hardness.

2. Method

2.1. Water potential test

A study was conducted in Cimarron Valley Research Station, Perkins, Oklahoma during 2020. Two varieties; Pawnee and Kanza were used. For each variety, three trees were selected and treated with three types of irrigation: full irrigation (normal rate of irrigation), half irrigation (half of normal rate) and no irrigation. Normally in Perkins, irrigation is applied at the rate of 0.73 gallon per min for 48 hours each week during August.

For stem water potential measurement, six leaves fully exposed to sunlight from each tree were selected and covered with aluminum foil for thirty minutes prior to measurement starting at 11:00 a.m. The measurements were taken by pressure chamber weekly in the month of August except two times a week in the first week of August. Furthermore, nuts were collected weekly from four directions of each irrigation trail tree from August until the harvest. We measured areas of shuck, shell and embryo using our collected nut samples. Area of nuts were measured by the used of Mask-RCNN as mentioned in Chapter 1. Besides, an extra three nuts from each irrigation trail tree were also collected to test the hardness of the shell. Hardness was tested by using the force gauge (Imada Co., LTD) with a 2mm diameter probe needle (Figure 3.3). Finally, grading was done at the time of harvest.

2.2. Shell firmness test

During the end of August, we collected six Kanza nuts which were damaged by the pecan weevil and each nut was divided into 12 sections as shown in Figure 6. There are two suture lines in pecan nut which is visible in the shell (Figure 3.6b) whereas in shuck region, there are four surfaces which are separated by faint or discolored lines. While in some cultivars, like Pawnee and Kanza, there is a no line on the fourth surface of the shuck region. There is no clarification for this appearance but research in English walnut, *Juglans regia*, has stated that the no line in shuck region is due to a difference between the initiation of two carpels (Shuhart, 1932). The shell region which have two suture lines lies exactly below adjacent of shuck region which have two discolored line surface. Moreover, nut is divided into two end; base end which is connected to stem and distal end where fruit set occur (Figure 3.6a). Because of this difference, it was possible to divide nut into 12 sections on nuts without damaging it. On each section the firmness was tested by using the force gauge (Imada Co., LTD) with a 2 mm diameter probe needle. The base end of the nut was marked as 1,4,7,10; the middle is marked as 2,5,8,11 and the distal end as 3,6,9,12 by holding the nut base up and distal down and moving in clockwise direction from shuck surface. While we collected the nut for first chapter, three extra nuts were also collected from each replication from both varieties, Pawnee and Kanza, from fruit set stage until the harvest of the nut for testing the hardness.

2.3. Data analysis

Data were analyzed in R 4.1.1 (R core team, 2021). Analysis of variance was performed and graphs were plotted by the use of ggplot package. Least significance difference (LSD) was conducted by the use of Agricole package. Pearson correlation coefficient test (r) was calculated to correlate shell area and the shell hardness.

3. Result and discussion

3.1. Irrigation

3.1.1 Water potential

Stem water potential of the no irrigation treatment was -13.3 MPa for Pawnee and -12.5 MPa for Kanza varieties, which was less than the corresponding varieties (-10.0 and -10.5 MPa, respectively) under the half irrigation treatments (Figure 3.4). Meanwhile, water potential for full irrigation at the end of August was -10.0 MPa for Pawnee and -7.8 MPa for Kanza. After the end of August, the orchard received rain of about one inch. The water potential measured after rainfall, increased drastically. For instance, Kanza treated with full irrigation, water potential reduced from -8.5 to -6.3 MPa. This data reveals that additional frequency of one or two irrigations during summer can alleviate drought stress in pecan trees. Also, the data reveals that the pressure chamber can be used efficiently for scheduling the irrigation of pecan trees (Scholander et al., 1965).

3.1.2 Nut Growth

Analysis of variance (ANOVA) was done to evaluate the impact on nut component (shuck, shell and embryo) for both varieties on each irrigation treatment (Table 3.1). In Pawnee variety, the area of embryo was not affected by irrigation treatment ($P = 0.0806$), whereas the shell and shuck were significantly affected by irrigation treatment ($P < 0.001$). Meanwhile for Kanza variety, the area of the embryo ($P = 0.002$) and the shell ($P < 0.001$) were significantly affected by irrigation treatment, whereas the shuck area was not influenced by irrigation ($P = 0.3$). Specifically, the full irrigation treatment for Kanza resulted in a larger embryo as compared to the half and no irrigation treatments (Table 3.2). The results suggest irrigation during the summer varies with cultivar in importance for the ovule expansion and embryo size (Sparks, 1995).

3.1.3 Shell firmness

The firmness of Pawnee and Kanza varieties showed non-significant difference among different types of irrigation (Table 3.3). Even though we found significant differences in the shell area for both varieties, the firmness was found to be not significantly different. Correlation between shell area and hardness in Kanza variety (Figure 3.5) revealed that the firmness of shell is not defined by area of shell. The similar pattern was observed in hazelnut as well (Valentini et al., 2015). Meanwhile, for the Pawnee variety there was a significantly positive correlation between shell area and hardness which was particularly higher for full irrigation (R^2 = 0.98). We analyzed this phenomenon in two ways since the firmness test and the area measurement did not use the same nuts. Within the same nut, it was hard to obtain consistent firmness throughout the length of the nut. Similarly, in hazelnut, the shell hardness was strongly correlated with the shell area but at the time of maturity shell hardness and area were negatively correlated (Valentini et al., 2015). Since our nut samples were collected from August until nut harvest, the overall combination of shell area and the hardness could have attributed to the difference in the ANOVA test.

Interestingly, the full irrigation treatment resulted in twice the number of white skins as compared to half and no irrigation in Pawnee. Similar responses were not observed for Kanza. These data reveal that the nut quality is determined by the irrigation during the summer month (Wells, 2015; Stein et al., 1989; Worley, 1982), but also depends upon the variety.

Ice damage during late October in 2020 reduced harvestability of the crop and limited findings from that year. We can infer that in some pecan cultivars irrigation can be reduced by half. As quality was seen to be improved only in Pawnee, it indicates that, utilizing the water availability for quality production also depends upon variety rather than irrigation alone.

3.2. Shell firmness of nut affected by weevils

The nut firmness value for both varieties was slow at beginning and rarely increased until the end of July, but firmness increased throughout the August and remain steady at the September (Figure 3.7). At the beginning of the growth, nuts were soft and green in color so the firmness was low. Following the August, firmness value starts to increase rapidly which is due to shell lignification (Valentini et al., 2015). In Perkins, August is the month where the nut enters three stages of nut: water, gel and dough stage. However, for the Pawnee variety the firmness decreased at the end of harvest. This might be because of the change in endocarp component of the shell (Caramiello, 1998; Guidone et al., 2007). The Kanza variety had higher firmness as compared to the Pawnee variety. For instance, in the last week of August, the firmness recorded for Pawnee is 20lb/2mm2 whereas for Kanza is about 40lb/2mm2.

The value of shell hardening varies among the individual nut but it gives us inference that weevil could oviposit the nut with weaker shell firmness (Figure 3.7). It is clear from Figure 3.8 that the firmness of shell in each section varied. The firmness value of section 3 and 9 is significantly higher than other section. Weevil damaged section in the graph is represented by an asterisk (*). Section 3 and 9 lies in the non-sutured end at distal region, whereas section 6 is at distal end of the suture. According to Smith & Mulder (2009), the weevil punctures in the distal end of the nut and our result seems to support this assumption. However, our research provides new additional information i.e., weakest point in nut is located at the suture region of shell and this information would help for further study on the suture (Zhang et al., 2020).

From Figure 3.8, most of the weevil damage is in the low nut firmness region (1, 6, 7, and 11) with section 11 being an exceptional with moderate nut firmness. This gives a clear image that the weevil oviposit in those region which have lower shell firmness. This experiment provides the possibility for future experiments on how to restrict the weevil ovipositional based on sectional firmness rather than growth time. Although this research is based on a small study on puncture of nut, larger number of nuts would be required to prove this phenomenon. Information about shell hardening or firmness can be used as a useful tool for orchard pest management. Furthermore, shell hardening information will provide information for breeder to increase tolerance or avoidance of the pest.

4. Conclusion

Irrigation of nut and the management of pecan weevil during nut maturity are two important factors that need to be considered during the fruiting season of the nut. Our results from irrigation highlights the importance of irrigation in summer and it facilitates in ovule expansion. Since some of the variety can tolerate the reduced amount of water, proper water reduction could be viable for some orchards. Whereas the weevil research highlights that the weevil oviposits in the weaker section of the nut; mostly in the sutured region. This information provides potential direction for further research on the suture region.

TABLES AND FIGURES

Figure 3.1. Kanza pecan at water stage.

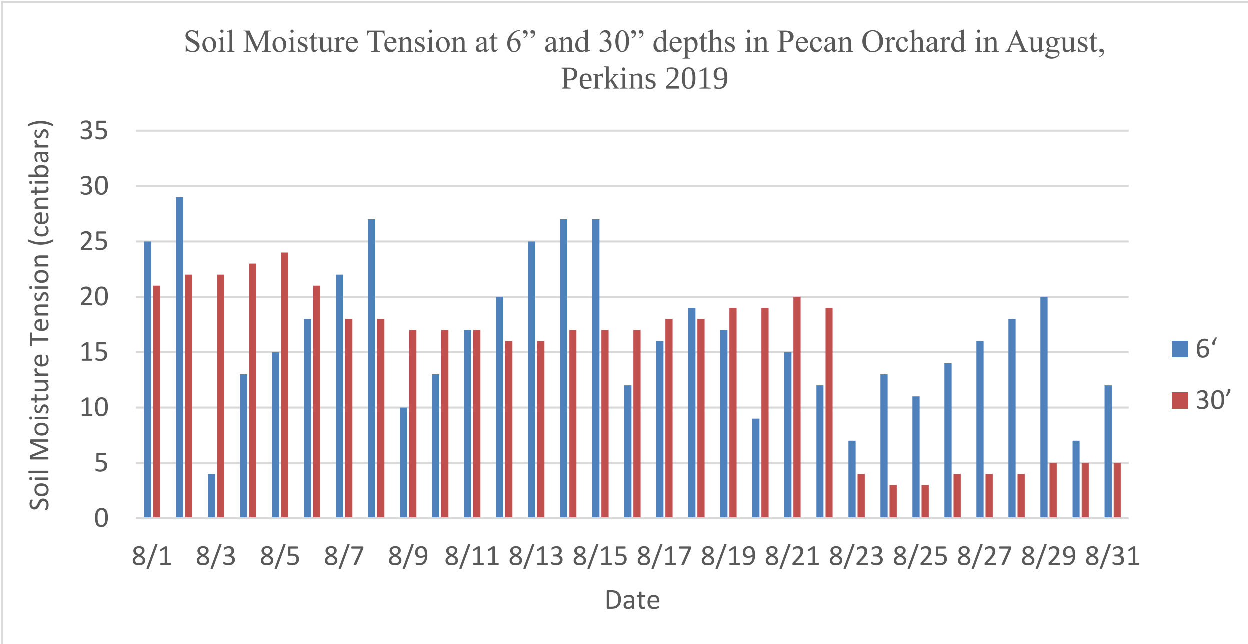

Figure 3.2. Soil moisture tension at 6’’ and 30’’ depths tested by WATERMARK soil moisture sensors installed at the distance to half canopy (Zhang et al., 2021)

Figure 3.3. Measuring pecan shell firmness using force gauge with a 2mm probe needle.

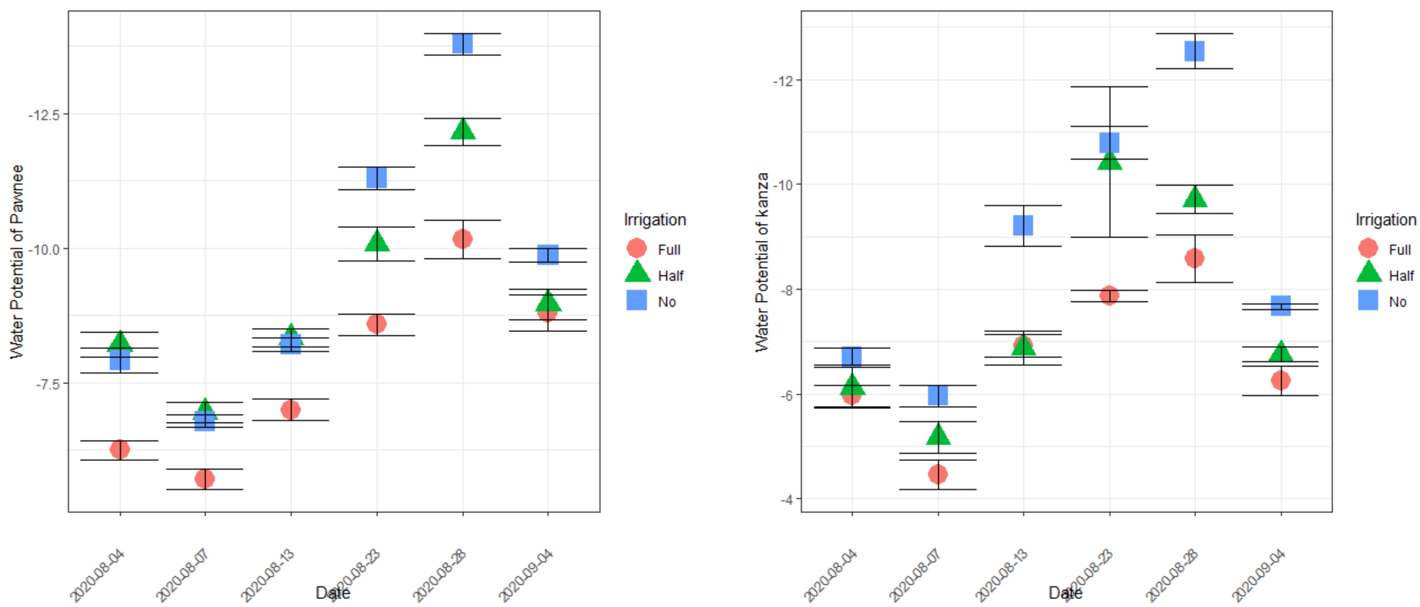

a b

Figure 3.4. Average leaf water potential (±Standard error) of Pawnee and Kanza trees tested once a week in August. Two tests in the first week. The red dots represent the full irrigation, green dots the half irrigation, and the blue is the non-irrigation. Note: water potential is a negative value, lower the negative value, higher demand for water.

Table 3.1. Analysis of variance for the area of the Pawnee and Kanza nut tested for different kind of irrigation treatment

Variety	Nut component	P-value
Pawnee	Embryo	NS
	Shell	<0.001***
	Shuck	0.00107*
Kanza	Embryo	0.00213**
	Shell	<0.001***
	Shuck	NS

* Significant at the 0.05 probability level; ** significant at the 0.01 probability level; *** significant at the 0.001 probability level; NS not significant

Table 3.2. LSD test for the Kanza area for different kind of irrigation treatment

	Type of irrigation	Mean embryo area (mm^2)
Kanza	Full irrigation	293.87a
	Half irrigation	280.78b
	No irrigation	275.06b

*Means within columns followed by the same letters are not statistically different at P=0.05

Table 3.3. ANOVA for the firmness of the Pawnee and Kanza nut tested for full, half and no irrigation

Variety	P-value
Pawnee	NS
Kanza	NS

* Significant at the 0.05 probability level; ** significant at the 0.01 probability level; *** significant at the 0.001 probability level; NS not significant

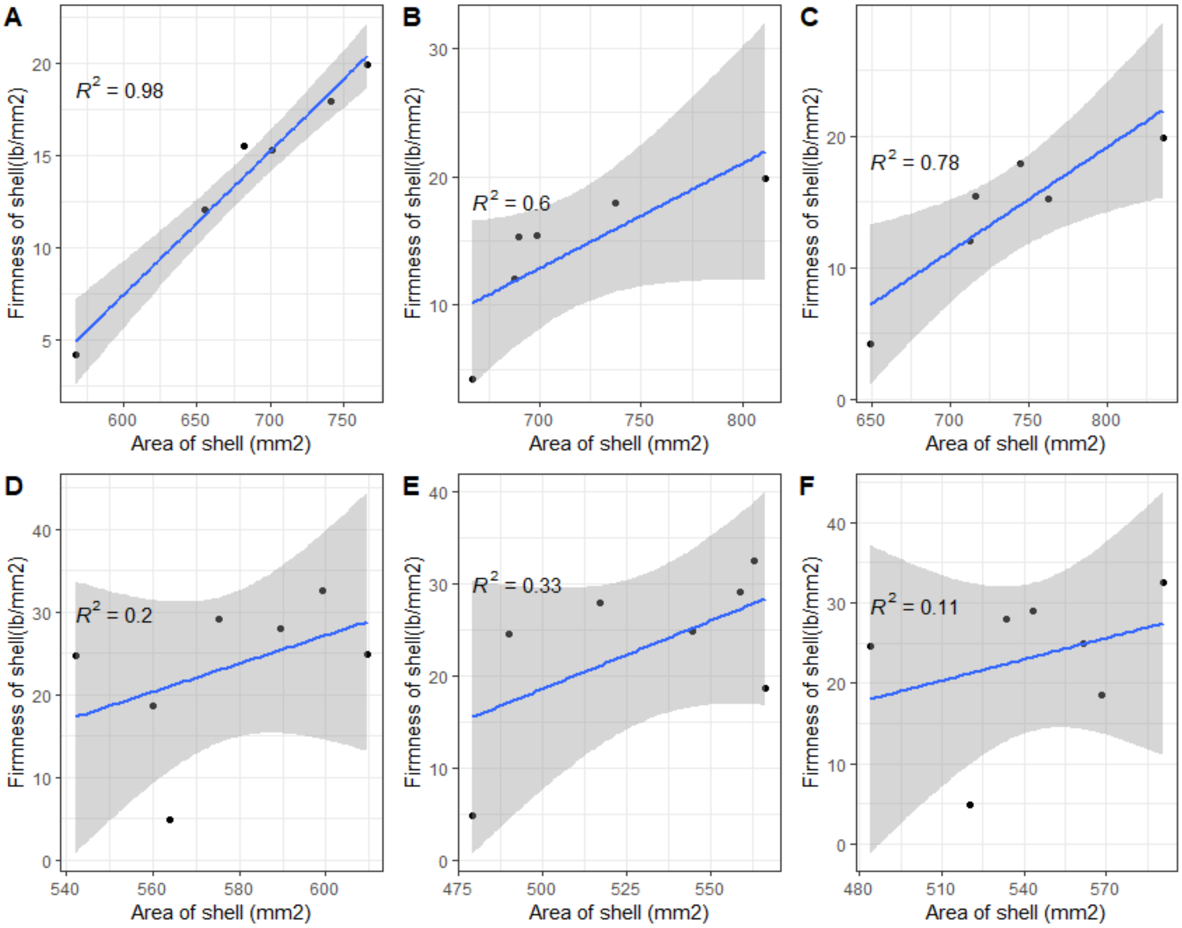

Figure 3.5. Correlation between shell area and shell hardness during the Pecan nut growth for Pawnee (A to C) and Kanza (D to F) variety with different irrigation treatment; A and D (Full irrigation), B and E (Half irrigation), and C and F (No irrigation). Shaded area is the of 95% confidence interval.

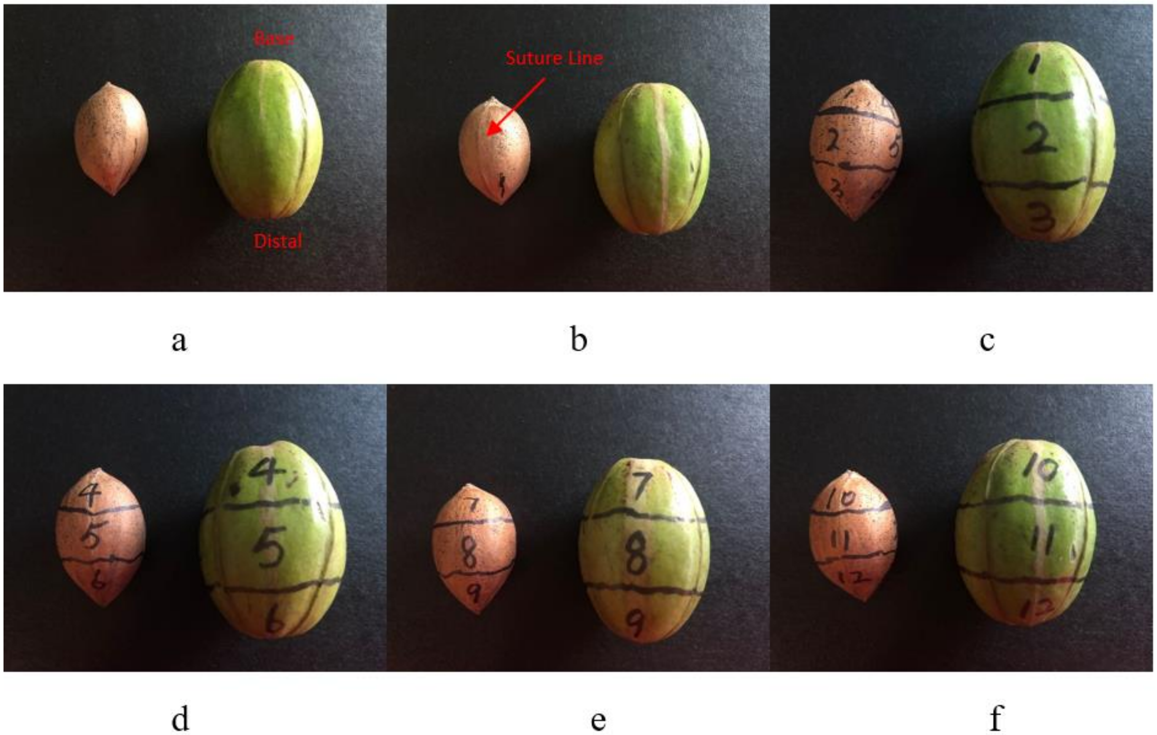

Figure 3.6. Kanza nuts with and without shucks (a) non-sutured side on shell, the middle of the shuck has faint discolored lines; (b) sutured side on the shell, the middle of shuck has clear discolored lines; (c) from base to distal ends divided into 1, 2, 3 sections on the shuck surface without discolored line; (d) from base to distal ends divided into 4, 5, 6 sections on the surface adjacent to (Figure 3.6c) in clockwise direction; (e) from base to distal ends divided into 7, 8, 9 sections on the surface adjacent to (Figure 3.6d) in clockwise direction; from base to distal ends divided into 10,11,12 sections on the surface adjacent to (Figure 3.6e) in clockwise direction.

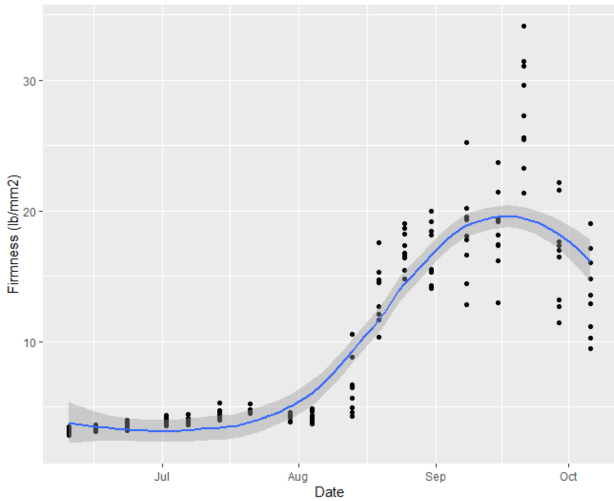

a

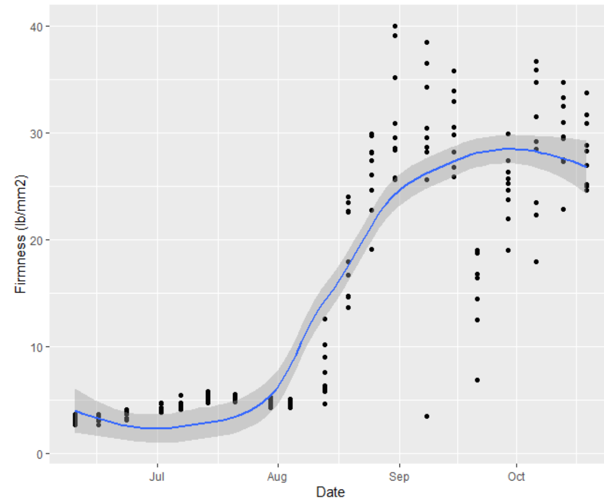

b

Figure 3.7. Growth curve for the shell firmness with confidence interval (sections 2 or 8) of Pawnee (a) and Kanza (b) nuts collected from early fruit set July through October in 2020.

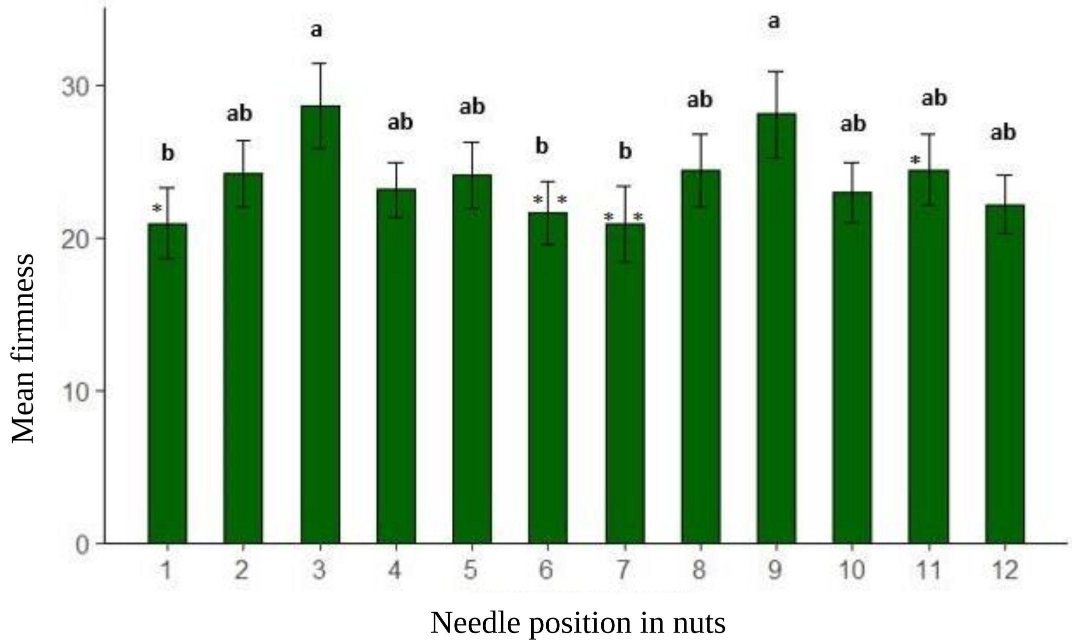

Figure 3.8. The mean nut firmness (±Standard error) (lb/2mm^2) of the 12 sections of the six nuts on which the asterisk (*) indicates sections with weevil damage. Different letters indicate significant statistical differences.

REFERENCES

Aardema, M., Miller, J., & Slavin, J. (2016). Dossier in Support of the Generally Recognized As Safe (Gras) Status of Pecan Shell Fiber As a Food Ingredient. In *Pecan Shell Fiber GRAS Notification* (Issue 646).

Alves, G., T. Ameglio, A. Guilliot, P. Fleurat-Lessard, A. Lacointe, S. Sakr, G. Petel, and J.L. Julien. 2004. Winter variation in xylem sap pH of walnut trees: Involvement of plasma membrane H^+-ATPase of vessel-associated cells. Tree Physiol. 24:99–105

Azarenko, A. N., Chozinski, A., & Brewer, L. J. (2008). Fruit growth curve analysis of seven sweet cherry cultivars. *Acta Horticulturae*, *795 PART 2*(August 2008), 561–565.

Bustan, A., Avni, A., Lavee, S., Zipori, I., Yeselson, Y., Schaffer, A. A., Riov, J., & Dag, A. (2011). Role of carbohydrate reserves in yield production of intensively cultivated oil olive (Olea europaea L.) trees. *Tree Physiology*, *31*(5), 519–530.

Byford, R. (2005). *Growth and Development of Pecan Nuts Guide H-618*.

Caramiello, R. (1998). Structure and characteristics of the hazelnut shell in different cultivars and their agronomic and industrail influence. *Proceedings of the XXV International Horticulture Congress: Brussels, Belgium,2-7*, *517*, 195 to 208.

Carroll, B., Smith, M. W., & Reid, W. (2015). *Pecan Crop Load Management*.

Chuine, I., Cour, P., & Rousseau, D. D. (1999). Selecting models to predict the timing of flowering of temperate trees: Implications for tree phenology modelling. *Plant, Cell and Environment*, *22*(1), 1–13.

Conner, P. J., & Worley, R. E. (2000). Alternate bearing intensity of pecan cultivars. *HortScience*, *35*(6), 1067–1069.

Costa, L., Ampatzidis, Y., Rohla, C., Maness, N., Cheary, B., & Zhang, L. (2021). Measuring pecan nut growth utilizing machine vision and deep learning for the better understanding of the fruit growth curve. *Computers and Electronics in Agriculture*, *181*(November 2020), 105964.

Da Silva, D., Qin, L., DeBuse, C., & DeJong, T. M. (2014). Measuring and modelling seasonal patterns of carbohydrate storage and mobilization in the trunks and root crowns of peach trees. *Annals of Botany*, *114*(4), 643–652.

Darbyshire, R., Webb, L., Goodwin, I., & Barlow, E. W. R. (2014). Challenges in predicting climate change impacts on pome fruit phenology. *International journal of of Biometeorology*, *58*(6), 1119–1133.

Dayan, E., van Keulen, H., Jones, J. W., Zipori, I., Shmuel, D., & Challa, H. (1993). Development, calibration and validation of a greenhouse tomato growth model: II. Field calibration and validation. *Agricultural Systems*, *43*(2), 165–183.

Donald Shuhart. (1932). Morphology and anatomy of the fruit of Hicoria pecan. *THE BOTANICAL GAZETTE*, *93*(1), 1–20.

Dozier, W. A., & Amling, H. J. (1974). Fruit Growth and Embryological Development of the STUART PECAN Carya illinoensis. *Agriculture Experiment Station/Auburn University*.

Fernandes, T. J., Pereira, A. A., & Muniz, J. A. (2017). Double sigmoidal models describing the growth of coffee berries. *Ciência Rural*, *47*(8), 1–7.

Godoy, C., Monterubbianesi, G., & Tognetti, J. (2008). Analysis of highbush blueberry (Vaccinium corymbosum L.) fruit growth with exponential mixed models. *Scientia Horticulturae*, *115*(4), 368–376.

Goldschmidt, E. E. (2018). An evolutionary platform for alternate bearing in fruit trees. *Acta Horticulturae*, *1229*, 1–7.

Goldschmidt, Eliezer E, & Golomb, A. (1982). The Carbohydrate Balance of Alternate-bearing Citrus Trees and the Significance of Reserves for Flowering and Fruiting. Journal of American Society for Horticultural Science, 107(2), 206–208.

Guidone, L., Valentini, N., Rolle, L., Me, G., & Tavella, L. (2007). Early nut development as a resistance factor to the attacks of Curculio nucum (Coleoptera: Curculionidae). *Annals of Applied Biology*, *150*(3), 323–329.

Harris, M. K. (1983). INTEGRATED PEST MANAGEMENT OF PECANS. In *Ann. Rev. Entomol* (Vol. 28).

He, K., Gkioxari, G., Dollar, P., & Girshick, R. (2020). Mask R-CNN. *IEEE TRANSACTIONS ON PATTERN ANALYSIS AND MACHINE INTELLIGENCE*, *42*(2), 386–397.

Herrera, E. A. (1990). Fruit Growth and Development of "Ideal" and "Western" Pecans. In *J. AMER. Soc. HORT. SCI* (Vol. 115, Issue 6).

Ito, A., Sakamoto, D., & Moriguchi, T. (2012). Carbohydrate metabolism and its possible roles in endodormancy transition in Japanese pear. *Scientia Horticulturae*, *144*, 187–194.

Kim, T., & Wetzstein, H. Y. (2005). Seasonal fluctuations in nutrients and carbohydrates in pecan leaves and stems. *Journal of Horticultural Science and Biotechnology*, *80*(6), 681–688.

Kishore, K. (2019). Phenological growth stages and heat unit requirement of Indian blackberry (Syzygium cumini L., Skeels). *Scientia Horticulturae*, *249*(February), 455–460.

Kozlowski, T. T. (1992). Carbohydrate sources and sinks in woody plants. *The Botanical Review*, *58*(2), 107–222.

Loescher, W. H., Mccamant, T., & Keller, J. D. (1990). Carbohydrate Reserves, Translocation, and Storage in Woody Plant Roots. *HortScience*, *25*(3), 274–281.

Mathanker, S. K., Weckler, P. R., Bowser, T. J., Wang, N., & Maness, N. O. (2011). AdaBoost classifiers for pecan defect classification. *Computers and Electronics in Agriculture*, *77*(1), 60–68.

McCutchan, H., & Shackel, K. A. (1992). Stem-water Potential as a Sensitive Indicator of Water Stress in Prune Trees (Prunus domestica L. cv. French). *Journal of the American Society for Horticultural Science*, *117*(4), 607–611.

Meade, K. A., Cooper, M., & Beavis, W. D. (2013). Modeling biomass accumulation in maize kernels. *Field Crops Research*, *151*, 92–100.

Miller, P., Lanier, W., & Brandt, S. (2001). Using Growing Degree Days to Predict Plant Stages. *Montana State University Extension Service*, *9*, MT00103 AG 7/2001.

Monselise, S. P., & Goldschmidt, E. E. (1982). Alternate Bearing in Fruit Trees. *Horticultural Reviews*, 128–173.

Mulder, P. G., Harris, M. K., & Grantham, R. A. (2012). Biology and management of the pecan weevil (Coleoptera: Curculionidae). *Journal of Integrated Pest Management*, *3*(1), 1–9.

Muniz, J. A., Nascimento, M. da S., & Fernandes, T. J. (2017). Modelos não lineares na descrição do crescimento de frutos de cacau com violações dos pressupostos. *Revista Caatinga*, *30*(1), 250–257.

Nzima, M. D. S., Martin, G. C., & Nishijima, C. (1997). Seasonal changes in total nonstructural carbohydrates within branches and roots of naturally “off” and “on” “Kerman” pistachio trees. In *Journal of the American Society for Horticultural Science* (Vol. 122, Issue 6, pp. 856–862).

Paine, C. E. T., Marthews, T. R., Vogt, D. R., Purves, D., Rees, M., Hector, A., & Turnbull, L. A. (2012). How to fit nonlinear plant growth models and calculate growth rates: An update for ecologists. *Methods in Ecology and Evolution*, *3*(2), 245–256.

Paul F. Smith. (1976). Collapse of “Murcott” Tangerine Trees. *Journal of American Society of Horticultural Science*, *101(1)*, 23–25.

Pavel, E. W., & DeJong, T. M. (1993). Relative Growth Rate and its Relationship to Compositional Changes of Nonstructural Carbohydrates in the Mesocarp of Developing Peach Fruits. *Journal of the American Society for Horticultural Science*, *118*(4), 503–508.

Peavey, M., Goodwin, I., & McClymont, L. (2020). The effects of canopy height and bud light exposure on the early stages of flower development in prunus persica (L.) batsch. *Plants*, *9*(9), 1–10.

Polito, V. S., & Pinney, K. (1999). Endocarp dehiscence in pistachio (Pistacia vera L.). *International Journal of Plant Sciences*, *160*(5), 827–835.

Prasad, A., & Sakai, K. (2015). Understanding the alternate bearing phenomenon: Resource budget model. *Chaos*, *25*(12).

Prusinkiewicz, P. (2004). Modeling plant growth and development. *Current Opinion in Plant Biology*, *7*(1), 79–83.

Qingbing, Z., Chengliang, L., Yubin, M., Shengwei, F., & Shiping, W. (2008). A machine vision system for continuous field measurement of grape fruit diameter. *Proceedings - 2008 2nd International Symposium on Intelligent Information Technology Application, IITA 2008*, *2*, 1064–1068.

Reginato, G.H., Callejas, R.H., Sapiaín, R.A., García-de-Cortázar, V., 2010. Rest completion and growth of 'Thompson Seedless' grapes as a function of temperatures. Acta Hortic. 872, 427–430.

Ribeiro, T. D., De Mattos, R. W. P., De Morais, A. R., & Muniz, J. A. (2018). Description of the growth of pequi fruits by nonlinear models. *Revista Brasileira de Fruticultura*, *40*(4), 1–11.

ROSECRANCE, R. C., WEINBAUM, S. A., & BROWN, P. H. (1998). Alternate Bearing Affects Nitrogen, Phosphorus, Potassium and Starch Storage. *Annals of Botany*, *82*(4), 463.

Salinas, I., Hueso, J. J., & Cuevas, J. (2019). Fruit growth model, thermal requirements and fruit size determinants in papaya cultivars grown under subtropical conditions. *Scientia Horticulturae*, *246*(December 2018), 1022–1027.

Singanusong, R., Mason, R. L., D'Arcy, B. R., & Nottingham, S. M. (2003). Compositional changes of Australia-grown Western Schley pecans [Carya illinoinensis (Wangenh.) K. Koch] during maturation. *Journal of Agricultural and Food Chemistry*, *51*(2), 406–412.

Smith, M. W., & Gallott, J. C. (1990). Mechanical Thinning of Pecan Fruit. HortScience, 25(4), 414–416.

Smith, M. W., & Mulder, P. G. (2009). Oviposition characteristics of pecan weevil. *Southwestern Entomologist*, *34*(4), 447–455.

Sousa, I. F., Kunzle Neto, J. E., Muniz, J. A., Guimarães, R. M., Savian, T. V., & Muniz, F. R. (2014). Fitting nonlinear autoregressive models to describe coffee seed germination. *Ciência Rural*, *44*(11), 2016–2021.

Spann, T. M., Beede, R. H., & Dejong, T. M. (2008). Seasonal carbohydrate storage and mobilization in bearing and non-bearing pistachio (Pistacia vera) trees. *Tree Physiology*, *28*(2), 207–213.

Sparks, D. (1974). The alternate fruit bearing problem in pecans. *65th Annual Report of the Northern Nut Growers Association Association*, *65*, 145–158.

Sparks, D. (1989). Drought Stress Induces Fruit Abortion in Pecan. *HortScience*, *24*(1), 78–79.

Sparks, D. (1995). Nut sizing period in pecan and soil water. *Northern Nut Growers Association*.

Sparks, D. (2005). Adaptability of pecan as a species. *HortScience*, *40*(5), 1175–1189.

Spicer, R. (2014). Symplasmic networks in secondary vascular tissues: Parenchyma distribution and activity supporting long-distance transport. *Journal of Experimental Botany*, *65*(7), 1829–1848.

Tixier, A., Gambetta, G. A., Godfrey, J., Orozco, J., & Zwieniecki, M. A. (2019). Non-structural Carbohydrates in Dormant Woody Perennials; The Tale of Winter Survival and Spring Arrival. *Frontiers in Forests and Global Change*, *2*(May), 1–8.

Tixier, A., Orozco, J., Roxas, A. A., Earles, J. M., & Zwieniecki, M. A. (2018). Diurnal variation in nonstructural carbohydrate storage in trees: Remobilization and vertical mixing. *Plant Physiology*, *178*(4), 1602–1613.

Tixier, A., Roxas, A. A., Godfrey, J., Saa, S., Lightle, D., Maillard, P., Lampinen, B., & Zwieniecki, M. A. (2017). Role of bark color on stem temperature and carbohydrate management during dormancy break in Persian walnut. *Journal of the American Society for Horticultural Science*, *142*(6), 454–463.

Tjørve, K. M. C., & Tjørve, E. (2017). The use of Gompertz models in growth analyses, and new Gompertz-model approach: An addition to the Unified-Richards family. *PLoS ONE*, *12*(6), 1–18.

Tommy E. Thompson. (1998). Soluble Solids Concentrations in Pecan Liquid Endosperm of Several Pecan Clones. *HortScience*, *33*(7), 1145–1146.

Tromp, J. (1983). Nutrient reserves in roots of fruit trees, in particular carbohydrates and nitrogen. *Tree Root Systems and Their Mycorrhizas*, *413*, 401–413.

Upson, S., Rohla, C., Locke, J., & Springer, J. (2012). PECAN PRODUCTION 101. Establishing and Managing an Improved Variety Pecan Enterprise in the Southern Great Plains. *The Samuel Roberts Noble Foundation Agricultural Division*, 5.

USDA-NASS. (2021). *Non-citrus fruits and nuts: 2006 summary* (Issue May).

Valentini, N., Moraglio, S. T., Rolle, L., Tavella, L., & Botta, R. (2015). Nut and kernel growth and shell hardening in eighteen hazelnut cultivars (Corylus avellana L.). *Horticultural Science*, *42*(3), 149–158.

Vesala, T., Sevanto, S., Grönholm, T., Salmon, Y., Nikinmaa, E., Hari, P., & Hölttä, T. (2017). Effect of leaf water potential on internal humidity and CO2 dissolution: Reverse transpiration and improved water use efficiency under negative pressure. Frontiers in Plant Science, 8(FEBRUARY), 1–10.

Wang, G., & Liu, X. (2004). Model Selection and Multimodel Inference. Second. NY: Springer-Verlag, 63(2020), 10.

Wells, L. (2015). Irrigation water management for pecans in humid climates. *HortScience*, *50*(7), 1070–1074.

Wong, B. L., Baggett, K. L., & Rye, A. H. (2003). Seasonal patterns of reserve and soluble carbohydrates in mature sugar maple (Acer saccharum). *Canadian Journal of Botany*, *81*(8), 780–788.

Wood, B. W., & McMeans, J. L. (1981). Carbohydrate changes in various organs of bearing and nonbearing pecan trees. *Journal of the American Society for Horticultural Science*, *106*(6), 758–761.

Zavalloni, C., Andresen, J. A., & Flore, J. A. (2006). Phenological models of flower bud stages and fruit growth of "Montmorency" sour cherry based on growing degree-day accumulation. *Journal of the American Society for Horticultural Science*, *131*(5), 601–607.

Zhang, B., Huang, W., Gong, L., Li, J., Zhao, C., Liu, C., & Huang, D. (2015). Computer vision detection of defective apples using automatic lightness correction and weighted RVM classifier. *Journal of Food Engineering*, *146*, 143–151.

Zhang, J., Ranford, T., & Taylor, C. (2015). Heat model for pistachio bloom and harvest. *Scientia Horticulturae*, *186*, 47-53.

Zhang, L., Laca, E., Allan, C. J., Mahvelati, N. M., & Ferguson, L. (2021). Nonlinear model selection for fruit and kernel development as a function of heat in pistachio. *HortScience*, *56*(7), 769–779.

Zhang,L., Panta,S., Maness,S., & Heerema, R (2021 September). Insight into Alternate Bearing: Do Carbohydrates Drive it? Pecan South? Volume 54, 16-19

Zhang,L., Panta,S., Massey.,Josh, & Saleh, Taghvaeian (2021 June). Irrigation management for Pecans at Water Stage. Pecan South. Volume 54, 16-19

Zhang,L., Panta,S., Seuhs.,Kelly, & Mulder,Phil (2020 November).OSU Study Links Nut Firmness and Weevil Infection. Pecan South. Volume 53, 12-17

VITA

Srijana Panta

Candidate for the Degree of

Master of Science

Thesis: **MODELING THE PECAN NUT GROWTH AND CARBOHYDRATE REQUIREMENT AND APPLICATION OF MODELS**

Major Field: Horticulture

Biographical:

Education:

Completed the requirements for the Master of Science in Horticulture at Oklahoma State University, Stillwater, Oklahoma in December, 2021.

Completed the requirements for the Bachelor of Science in Agriculture at Tribhuvan University, Kathmandu, Nepal in 2018.

Experience:

Graduate Research Assistant
Oklahoma State University, Stillwater, Ok
Department of Horticulture and Landscape Architecture

Professional Memberships:

American Society for Horticultural Science (ASHS)
Oklahoma Pecan Growers Association (OPGA)